Niels Bohr Institute

LUND UNIVERSITY

Department of Physics

A Case Study of Hurricane Sandy

-According to ERA-Interim

A Bachelor's Thesis in Meteorology

Marie Staerk

Copenhagen University; Niels Bohr Institute
Lund University; Department of Physics

June 12, 2013

Supervisor: Aksel Walløe Hansen, NBI
Examiner: Peter Aakjær, DMI
Examiner: Carl-Erik Magnusson, LU

Abstract

In late October 2012 hurricane Sandy caused a lot of damage to the islands in the Caribbean Sea and later on (as an extratropical cyclone) to the United States; New Jersey. The system was different in many ways relative to "normal" hurricanes, e.g. its track, its lack of eye at times it was classified as a hurricane and its great size which all partly was due to the prevailing circulations in the upper troposphere at the time being. It was the interaction with an upper level trough that made Sandy to reintensify before she made landfall in New Jersey which resulted in a severe storm surge. Sandy got a lot of attention in media, which started to refer her as the "Frankenstorm", a very suitable nickname.

In this thesis it is investigated when Sandy experienced mostly baroclinic or barotropic features with the help of the reanalysis system ERA-Interim. Whether a weather system experiences baroclinic or barotropic features depends on the surrounding environment. This interaction between Sandy and her surroundings is treated in the Case Study which also covers why Sandy obtained the track that she did and why she did not experience an eye at certain times.

To be able to see how well the reanalysis performed on Sandy a comparison of i.e. mean sea level pressure (MSLP) and maximum sustained winds is made between the obtained values from ERA-Interim and the best estimates of Sandy presented by the National Hurricane Center (NHC). The values differ to quite a great extent (where the values from ERA-Interim underperform) and the reasons for that are mostly due to the coarse resolution of the reanalysis but also due to that ERA-Interim does not make use of all available observations from satellites. However, the overall tendencies of Sandy's track and MSLP were captured by ERA-Interim.

Table of Contents

1 Introduction

Few tropical cyclones have brought so much attention to the rest of the world as Sandy did in late October 2012. The system developed over the southern Caribbean Sea, moved towards the north and hit Jamaica as a category 1 hurricane and eastern Cuba as a category 3 hurricane. Thereafter the system lost some intensity but still passed the southern parts of Bahamas as a category 1 hurricane. While over Bahamas Sandy started to undergo a complex evolution which made her to grow in size and the system continued to weaken and became a tropical storm north of the islands. After Sandy had passed Bahamas she made a turn towards northwest and regained force over the Atlantic Ocean and once again she became a hurricane. While approaching the United States she moved over colder water and interacted with an upper level trough. This caused Sandy to weaken and hit United States; New Jersey as an extratropical (post-tropical) cyclone. However, even though Sandy made landfall as an extratropical cyclone she caused a lot of damage to the United States and the preliminary estimates is that she has cost more than $50 billion. The damage was mostly due to her large horizontal extension which caused her to bring a catastrophic storm surge, especially to the coastlines of New Jersey and New York [Blake *et al*, 2013]. Sandy was a rare system in multiple ways, for instance the deviant origin, the fact that she did not have an eye even though she was classified as a hurricane and her large horizontal extension.

Reanalysis, i.e. estimates of the actual state of the atmosphere is often used in different meteorological and climate research projects. For instance the *European Centre for Medium–Range Weather Forecasts* (ECMWF) has used reanalyses to recreate how the weather was on the days before and on the historical D-day, in early June 1944. Even though the reanalyses used for this purpose were not as sophisticated as the reanalysis systems are today, it resulted in a good overview of the weather, compared with actual observations [ECMWF, May, 2013].

Sometimes people take reanalyses to be more or less equivalent with actual observations but one has to be careful by doing so since that almost never is the case. The higher resolution of the reanalysis the better the estimates get, but it can still deviate from how the actual state was. Actual observations are used when producing reanalyses, the more observations, the better reanalyses. Since the introduction of weather satellites in the late 1960’s the amount of observations have increased enormously and provided both better forecasts and reanalyses [Dee *et al*, 2011].

In this thesis it is investigated whether reanalyses can capture Sandy’s path and the system’s meteorological state or not. It has been chosen to work with ECMWF’s reanalysis system, ERA-Interim, using a grid size with the resolution 0.75x0.75 (of a degree grid). This is not the greatest resolution that is publicly available from ECMWF, but it is not the worst resolution either. Relevant parameters are downloaded, decoded and displayed as plots with the help of the *Grid Analysis and Display System* GrADS). The resulting plots and data are then used to make a case study for Sandy and also for a comparison between the ERA-Interim values and the best estimates of Sandy produced by the *National Hurricane Center*

The report starts with some relevant theory about tropical cyclones and extratropical cyclones (e.g. temperature structure and how the different systems gain their energy) and the extratropical transition. Thereafter the theory part continues with a section about the ERA-Interim System and one about forecasting Sandy. Under *Results* the case study is presented as well as the comparison between ERA-Interim and the best estimates from the *National Hurricane Center* (NHC). In the *Discussion* some different reasons for the deviating results are presented as well as difficulties of producing reanalysis with greater resolution.

2 Theory

2.1 Tropical Cyclones

Tropical cyclones are axisymmetric rotational systems that form in the tropics, normally at least 5° poleward due to the need of a sufficiently large value of absolute vorticity [Emanuel, 2003]. The tropical cyclones in the Atlantic Ocean often form on an "easterly wave" originating over North Africa. They start out as tropical disturbances which are unorganized system with heavy thunderstorms. If favourable conditions are met over a sufficiently long period of time so that enough energy and rotation are gained, this tropical disturbance may organize into tropical cyclones [MetEd, 2010]. The tropical cyclones with maximum winds of 33ms^{-1} or greater are called hurricanes, severe tropical cyclones or typhoons depending on the geographical location.

There are several ways to define a tropical cyclone but the most common way to define it is to categorize the cyclone by its maximum winds, averaged over a time period of ten minutes at a height of 10m. However, in the United States it is more conventional to average over one minute instead of ten as in the rest of the world. There are three different ranges to classify a tropical cyclone by its maximum wind speed v;

- Tropical depressions are a tropical cyclone with $v < 17$ms^{-1},
- Tropical storms occur when $18 < v < 32$ms^{-1},
- and when the maximum winds exceed 33ms^{-1} the system is called a hurricane.

The classification system described above is used in the western North Atlantic and in the eastern North Pacific regions.

Considering the North Atlantic basin, tropical cyclones generally form in the southeastern part of the basin and move westward and slightly poleward. Generally the hurricane dissipates when moving over colder water or make landfall. If the tropical cyclone does not make landfall it typically recurves east- and poleward and becomes a part of the westerlies [Emanuel, 2003]. Below are two plots showing the probability of a hurricane to affect a certain area. The left plot shows the probabilities during the whole hurricane season, i.e. first of June to last of November while the right plot shows the probability of occurrence of a hurricane during October. The data is based on analyses from the period 1944 to 1999 [NOAA/National Hurricane Center. January, 2010].

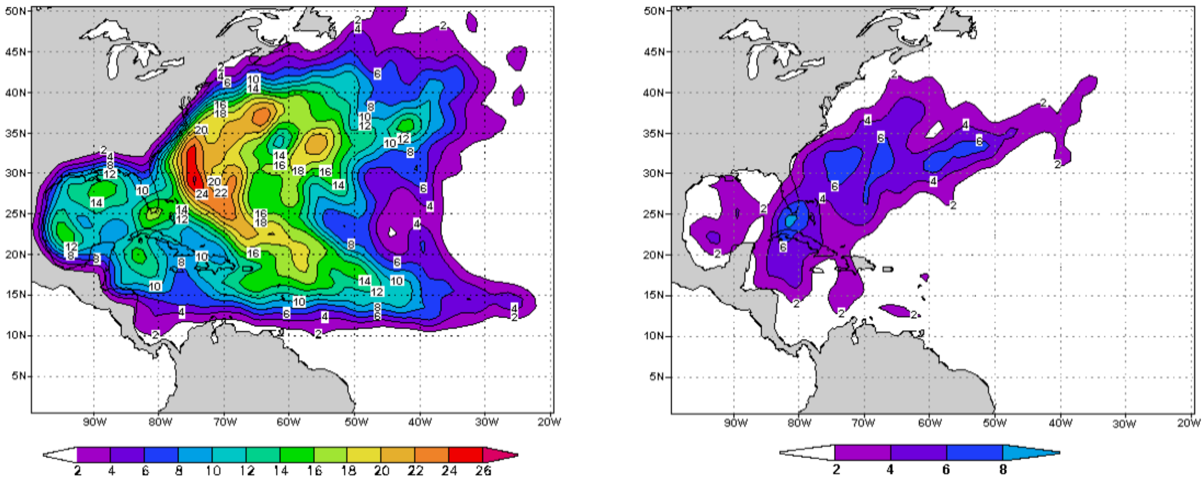

Figure 1 illustrates the probability of a hurricane to affect a certain location. The left plot shows the probability during the hurricane season and the right the probability of occurrence in October. The plots are consistent with the theory of how hurricanes generally move. However, these plots just show the probabilities for hurricanes and not the occurrence of e.g. a tropical storm or extratropical lows originating from hurricanes [NOAA/National Hurricane Center. January, 2010].

2.1.1 Formation and energetics of Hurricanes

Modelling tropical cyclones shows that they may develop spontaneously as long as there is a combination of a sea surface temperature that is high enough and a rotation that is strong enough. Comparing those modelled values with the ones observed in the real troposphere one finds that the values in reality are too low for hurricanes to develop spontaneously. This means that some additional trigger is needed to initiate a tropical cyclone. The trigger can be of different nature but it is always a preexisting disturbance in the troposphere. About 10% of the tropical cyclones over the world form and develop over the North Atlantic Ocean where the preexisting disturbance commonly is a 100-km-scale "easterly wave". The wave usually forms over the sub-Saharan Africa and then starts to move in a westerly direction over the Atlantic Ocean [Emanuel, 2006].

Little is known about the genesis of hurricanes but some necessary conditions are that the sea surface temperature need to exceed 26°C and further that the vertical wind shear is weak (less than $10ms^{-1}$ from the surface to the upper levels of the troposphere). Additionally there needs to be a low-level disturbance with enough convergence and vorticity and that the temperature declines sufficiently fast with height so that a moist air parcel can remain positively buoyant throughout a deep layer. The last criterion is needed for the creation of thunderstorms. Since it is the thunderstorm activity that allows the heat stored in the ocean to be released in the troposphere and thus helps the development of a hurricane this is a necessary condition [NOAA/National Hurricane Center. 23rd of May, 2013].

Once a tropical cyclone has developed the primary energy source is heat transfer from the ocean to the overlying air, accomplished by evaporation of seawater. The energy cycle of a mature hurricane is comparative with that of an ideal Carnot engine. The working fluids in the imaginary engine are a mixture of water vapour, dry air and suspended condensed water which all are in thermodynamic equilibrium. The power to the energy cycle comes from the temperature difference between the sea surface and the overlying air. The difference, or the thermal disequilibrium, allows heat flux from the tropical ocean to the air. The heat transfer from the ocean to the overlying air is mostly accomplished by evaporation, which in turn has a large heat of vaporization. A necessary condition for maintaining the evaporation is that the air a short distance above the sea surface must be dry, much drier than it would be if the air and the sea surface were in thermodynamic equilibrium.

Figure 2 illustrates the working scheme of an idealized hurricane Carnot engine [Emanuel, 2006]. The figure illustrates a cross section and it may look like that the air parcel moves straight towards the centre but it actually slowly spirals towards the centre in a cyclonic sense. Imagine that an air parcel needs to move from point A to A to complete the energy cycle. Through the cyclic process the air parcel will undergo several phase changes but it will return to its initial state which means that the work (internal in the case of a hurricane) done is due to the net heat input. This arises from the *First Law of Thermodynamics*;

$$\Delta u = q - w, \tag{1}$$

where Δu is the change in internal energy (which equals zero in the case of a cyclic process), q is the heat transferred (in this case mostly accomplished through evaporation) and w represents the work done. Assume that during one cyclic process a quantity of heat, Q_1 is absorbed by the working substance and another quantity of heat, Q_2 is rejected, then the work done by the engine is $Q_1 - Q_2$ [Wallace and Hobbs, 2006].

From point A to B the air parcel flows from higher to lower pressure, from the outer regions of the hurricane (to the right in the figure) to the centre of it (to the left in the figure). The air parcel is in contact with the sea surface (a large heat reservoir) and it undergoes a nearly isothermal expansion as it flows towards the centre.

In the mature hurricane air spirals in towards the centre close to the surface and due to conservation of angular momentum air will rotate faster close to the vortex's axis.

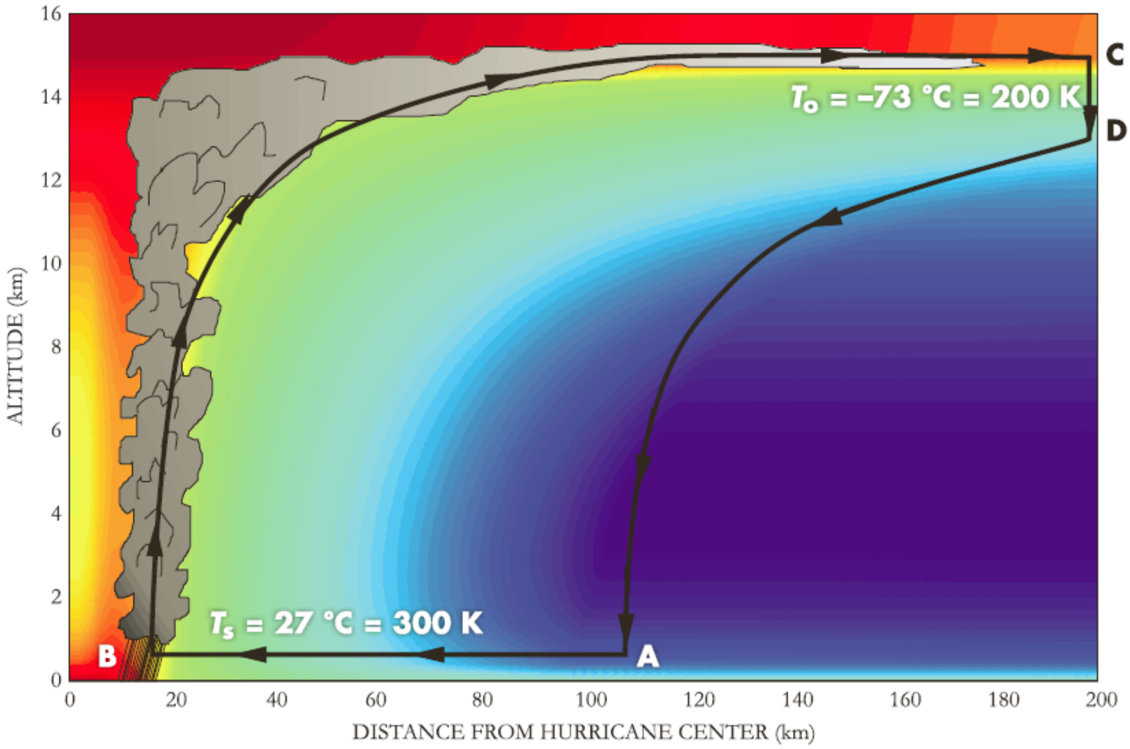

Figure 2. Illustration of a mature hurricane whose energy cycle works as a Carnot engine. The colours designates entropy where the blue indicates lower values than the red colour. Entropy, s, is a conserved quantity while it undergoes adiabatic displacements with air. Entropy is approximately defined as; $s \approx C_p \ln(T) - R_d \ln(p) + L_v q/T + qR_v \ln(H)$*, where* C_p *is the heat capacity at constant pressure, T is the absolute temperature,* R_d *and* R_v *is the gas constant for dry air and water vapor, p is pressure,* L_v *is the latent heat of vaporization, q is the concentration of water vapor and H is the relative humidity* [Emanuel, 2006].

The entropy increases towards the eyewall and is a measure of disorder in the system. The increase is due to the increase in enthalpy[1] transfer from the sea to the overlying air (the enthalpy transfer is mostly accomplished through evaporation of seawater). The increase in entropy is also due to dissipation of kinetic energy in the planetary boundary layer [Emanuel, 2006]. The far most important sink of kinetic energy occurs between A and B, due to friction between the ocean and the overlying air which in turn decreases the angular momentum.

When the air parcel reaches point B in the figure it starts to ascent (towards lower pressures) in a nearly adiabatic manner along lines with more or less constant entropy and angular momentum. Point B represents the location with the strongest winds, which typically occur 5-100 km from the centre of the hurricane. The air parcel ascends from point B to C creating the great cumulonimbus and the characteristic eyewall [Emanuel 2003].

An assumption must be made at point C to make it possible to close the Carnot cycle. In a real storm this never happens due to exchange with the environment and the air parcel leaves the system and gets incorporated into other weather systems. However, in simulated storms it is possible to close the cycle. Since numerically simulated axisymmetric storms

[1] Enthalpy is defined in the following way; $H = u + p \cdot V$ and is a measure of the total energy in a thermodynamic system, where p represents pressure and V volume. By making use of the first law of thermodynamics one can derive an expression for heat transfer (change in enthalpy), provided that it occurs under constant pressure, which states that: $H_2 - H_1 = C_p \cdot (T_2 - T_1)$, where $C_p$is some heat capacity coefficient [NASA, 2008].

behave very much like real storms, it validates this idealisation of a closed cycle. The assumption that needs to be made is to allow the gained entropy (heat) from the ocean to be radiated to space as electromagnetic radiation. As the air parcel cools it will become negatively buoyant towards its surroundings and it will start to descend. The continuous radiation allows the air parcel to descend in a nearly isothermal way from C to D [Emanuel, 2006]. Angular momentum is gained by the air parcel in this leg through mixing with the environment. To be able to complete the cycle the air parcel needs to move from D to A. The air parcel does so through adiabatic compression in an angular-momentum-conserving way. Entropy is both lost and gained between the two points but only little or no kinetic energy is generated. This is due to that the (irreversible) entropy source is produced by mixing of dry and moist air (with roughly the same temperature).

To summarize the sequence of events; the air parcel starts with undergoing an isothermal expansion (with addition of enthalpy) between A and B which is followed by an adiabatic expansion between point B and C. Thereafter the air parcel is a subject to isothermal compression and during the last leg adiabatic compression. This is exactly what happens in the cyclic process of the ideal Carnot engine. However, there is one essential difference between the energy cycle of the mature hurricane and the Carnot engine and that is how the created energy is used. In the latter one it is used to do work on its environment and in the former one it is used up in the boundary layer and turned back to heat through turbulent dissipation [Emanuel, 2003].

The efficiency, η, of the ideal Carnot engine is defined as;

$$\eta = \frac{\text{Work done by the engine}}{\text{Heat absorbed by the working substance}} = \frac{Q_1 - Q_2}{Q_1}. \quad (2)$$

[Wallace and Hobbs, 2006].

It is possible to derive an expression for the net production of mechanical energy in a hurricane and the complete derivation was first accomplished by Bister and Emanuel, 1998. An approximate derivation was later developed by Emanuel and was presented in Emanuel, 2003 and is the one described below;
Most of the heat input but even the dissipation of the generated kinetic energy in a hurricane occurs through the different transfers between the sea surface and the overlying air. The flux of enthalpy from the sea to the air and the flux of momentum into the sea may be quantified by using bulk formulas in the following form;

$$F_k = C_k \rho |V| (k_0^* - k) \quad (3)$$

and

$$F_m = -C_D \rho |V| V. \quad (4)$$

ρ is the density of air, V is the wind close to the surface, k_0^* is the enthalpy of air at the air-sea interface which is assumed to be saturated with water vapour at temperatures corresponding to the temperature of the ocean, k is the specific enthalpy[2] of air near the surface. C_k and C_D are the (dimensionless) transfer coefficients of enthalpy and momentum.

Further it is possible to model the vertically integrated dissipative heating of the boundary layer as;

$$D = C_D \rho |V|^3. \quad (5)$$

[2] The specific enthalpy h (in the text k) is obtained by dividing the enthalpy with the mass and one obtains the expression: $h_2 - h_1 = c_p \cdot (T_2 - T_1)$, where c_p represents the specific heat capacity at constant pressure [NASA, 2008].

The net production of mechanical energy in the ideal hurricane Carnot engine is obtained by;

$$P = 2\pi \frac{T_s - T_c}{T_s} \int_a^b [C_k \rho |V| (k_0^* - k)] + C_D \rho |V|^3 r dr, \tag{6}$$

where T_s represents the sea surface temperature and T_c represents the mean temperature in point C, the cold source of the engine (where heat is rejected through IR-radiation). The integral is taken from point A to B since this is the only leg adjacent to the sea and where most energy is created. However, it occurs net energy dissipation as well as net mechanical energy production which is described by the following formula,

$$D = 2\pi \int_a^b C_D \rho |V|^3 r dr. \tag{7}$$

One is able to obtain an approximate expression for the maximum wind speed by equating the two above equations and by making the assumption that both the integrals are dominated by the values of their integrands close to the radius of maximum wind speed;

$$|V_{max}|^2 \approx \frac{C_k}{C_D} \frac{T_s - T_c}{T_c} (k_0^* - k). \tag{8}$$

Despite that the above expression is an approximation one gets the same result when doing the whole derivation, which can be seen in Bister and Emanuel, 1998. The interesting thing about the above equation is the middle term on the right hand side. This term is similar to eq. (2) which describes the efficiency of the Carnot engine, but in the denominator the temperature of the rejected heat has replaced the temperature of the absorbed heat. This difference reflects the added contribution of dissipative heating that occurs in hurricanes [Emanuel, 2003].

2.1.2 The Structure and the Eye of a Hurricane

A very characteristic feature of many hurricanes is the cloudfree region in the centre of the storm, the eye. The radius of the eye typically ranges between 30-60km but it may be as small as 8km across and it may be as large as 200km across [NOAA, National Hurricane Center, 20th May 2011]. The eye is created in a process where the maximum upflow occurs within the eyewall, creating powerful cumulonimbus [Emanuel, 2003]. The most intense convection and strongest winds typically occur at a radius less than 100km from the centre. This fact validates to classify hurricanes as mesoscale systems even though that the radial scale can be several hundred kilometres [Holton, 2004].

The genesis of the eye is not yet fully understood but some theories are more accepted than others. The two most accepted theories for eye formation suggest the following;

- that the subsidence in the eye is caused by that the (radial) tangential wind field spreads and/or decays with height, at levels where approximate gradient wind balance prevails. This results in an adverse perturbation pressure gradient which induces subsidence. This subsidence is almost counteracted by an upward directed buoyancy force caused by that the air in the eye is much warmer than its surroundings. The net result is however that air slowly subsides in the eye [Smith, 1980].
- that the eye forms due to the latent heat release in the eyewall which forces subsidence in the eye.

It is also possible that eye formation is a combination of above theories. However the result is the same which is that air subsiding, in the eye, with velocities of 0.05-0.1ms^{-1}. The air compresses and warms relative to the air in the eyewall and creates a warm core system [NOAA/National Hurricane Center. May, 2011].

Outside the eyewall of cumulonimbus air is subsiding as well, but in this area there can exist columns of rising air (but slower that within the eyewall) creating spiral bands of cumulonimbus clouds, often with very heavy showers [Emanuel, 2003]. The rainbands slowly spiral counterclockwise (cyclonic) around the hurricane and often connect to the eye wall. The length of these bands often extends a few hundred kilometres from the eye wall while their width normally ranges from a few to tens of kilometres [NOAA/National Hurricane Center. May 4th, 2013].

A warm core system

One can easily imagine from above section that hurricanes are warm core system since air is subsiding in the eye and thus warming the air. However, below follows a more comprehensive explanation derived in *An Introduction to Dynamic Meteorology*, Holton, 2004;
The thermal wind in an axisymmetric hurricane can be derived from the gradient wind balance expressed in cylindrical coordinates and be expressed in the following way;

$$\frac{v_\lambda^2}{r} + f v_\lambda = \frac{\partial \Phi}{\partial r} \quad (9)$$

where v_λ represents the tangential velocity, which is positive in an cyclonic manner (anticlockwise) and r represents the radial distance from the pressure centre (or axis of the storm) which is positive in the outward direction. The tangential velocity, v_λ, can be replaced with the absolute angular momentum, M_λ. This is of interest in this case since when following the motion the absolute angular momentum is nearly conserved above the planetary boundary layer whilst the tangential velocity is not. The tangential velocity and absolute angular momentum is interrelated by the following expression, $M_\lambda \equiv v_\lambda r + f r^2/2$, where f is the Coriolis parameter. The first term on the right hand side is the contribution from the rotating wind field whereas the second is the contribution of Earth's rotation. Equation (9) can thus be expressed as (see appendix *Derivations* for the whole derivation):

$$\frac{M_\lambda^2}{r^3} - \frac{f^2 r}{4} = \frac{\partial \Phi}{\partial r} \quad (10)$$

It is more interesting in this case to eliminate the geopotential height, Φ, and replace it with something that expresses temperature. This can be done with the help of the hydrostatic equation (in log-pressure coordinates):

$$\frac{\partial \Phi}{\partial z^*} = \frac{RT}{H} \rightarrow \partial \Phi = \partial z^* \cdot \frac{RT}{H} \quad (11)$$

The above expression can be used together with equation (10) to obtain a relationship between the vertical shear of the absolute angular momentum and the radial temperature gradient:

$$\frac{1}{r^3} \frac{\partial M_\lambda^2}{\partial z^*} = \frac{R}{H} \frac{\partial T}{\partial r} \quad (12)$$

Observations have shown that the maximum cyclonic flow in hurricanes is the greatest near the top of the boundary layer. Since the absolute angular momentum is conserved above the boundary layer it means that $\partial M_\lambda / \partial z^* < 0$ here. If the equal sign in equation (12) should be fulfilled, then $\partial T/\partial r < 0$. Since r is defined as positive radially outward, then the temperature needs to decrease while moving away from the centre of the hurricane. This means that theory and observations predict the same temperature structure of hurricanes, that they are warm core systems with a maximum of temperature in the pressure centre [Holton, 2004].

Winds

The winds in the centre of the hurricane are very calm but increase rapidly in strength while moving away from the centre. The winds reach maximum strength approximately 50-100km from the pressure centre. While moving further away from the centre the winds gradually decrease with increasing radius. This decrease follows a $r^{-1/2}$ decay law near the radius with maximum winds, but falls off more rapidly the further away from the pressure centre one gets. As one reaches a radius off between 100 up to 1000km it is no longer possible to distinguish the winds (according to strength) in the hurricane from the winds normally found in the tropics. The strongest winds are located close to the surface and decrease in magnitude the higher up one gets, until they finally reverse direction (to anticyclonic) at the top of the hurricane [Emanuel, 2006].

In general one finds the strongest wind in a hurricane on its right side relative to its movement. This arises from the fact that both the steering wind and the anticlockwise winds in a hurricane contribute to the wind on the right side. On the left side those two winds counteract each other. However, sometimes the strongest winds are observed on the left side [MetEd, 2013].

2.2 Extratropical Transition

If the hurricane curves and moves poleward (in the Atlantic Basin) it will either decay when moving over colder water or undergo an extratropical transition. Around 50% of the hurricanes in this area are transformed to extratropical cyclones. Whether they undergo the transition or not depends on the surrounding environment. During the early part of hurricane season extratropical transitions will occur further south than in the later months. This depends on that the required sea surface temperature for hurricanes to survive (T>26°C) extends further to the north during the later months. This means that the probability for a hurricane to undergo an extratropical transition increases during the later months due to the increased probability of interaction with the midlatitude jet stream. Interaction between a hurricane and a midlatitude jet stream or an upper level trough is a very favourable condition for extratropical transition.

When a tropical cyclone moves into an area where midlatitude weather conditions prevail it will meet conditions that are not favourable for hurricanes e.g. strong vertical wind shear but also lower sea surface temperatures. When the interaction starts the characteristics of the hurricane change dramatically e.g. the axisymmetric appearance disappears and the system takes the shape of an extratropical cyclone. The evolving extratropical (post-tropical) cyclone generally increases considerably in size and the strongest winds and heaviest precipitation that before were located in the eyewall are now more widespread in the weather system. If the extratropical transition occurs due to interaction with the downstream part of an upper level trough, the chances of rapid deepening and development increase. Rapid development of the extratropical cyclone results in strong winds (that even can reach hurricane force) over the ocean which can cause storm surge to nearby coastlines and further to heavy precipitation [Jones *et al,* 2003].

2.3 Extratropical Cyclones

Due to the differential heating of Earth by the Sun, a temperature gradient is created over the Earth, with the highest temperatures in the south and the lowest in the north (it is only the northern hemisphere that is concerned in this thesis). This temperature gradient gives rise to atmospheric motions on very different length scales including eastward propagating midlatitude westerly jet streams that are located close to the top of the troposphere. The jet streams are essential to the weather on the middle latitudes and one often finds eastward propagating baroclinic waves superimposed on them. These waves gain their energy from the temperature gradient and further tend to decrease the strength of this gradient, acting to smoothen out the temperature differences across the middle latitudes. The baroclinic waves belong to the category of weather systems that tend to be created more or less spontaneously due to instabilities in the large-scale flow pattern that they are embedded in. The flow in the lower levels of a baroclinic wave is the one associated with extratropical cyclones [Wallace and Hobbs, 2006].

2.3.1 Structure and Genesis of Extratropical Cyclones

The horizontal scale of extratropical cyclones is a factor 10 greater than that of hurricanes, 10^6m compared to 10^5m which makes them to be synoptic scale weather systems. Further they do not experience such an axisymmetric flow as hurricanes do and they generally exist for a shorter period of time compared to the tropical cyclones. When dealing with extratropical systems one often works in the quasi-geostrophic (QG) system. The QG system uses simplified dynamic equations for the atmosphere which contain several assumptions e.g. that the horizontal wind field is nearly geostrophic and that vertical velocities are much weaker than the horizontal wind field. The QG system was developed in order to achieve easier interpretation of the continuously evolving atmosphere (on synoptic scale) for instance with the help of the omega and the geopotential height tendency equations [Holton, 2004].

Genesis of an extratropical cyclone

In contrast to the genesis of tropical cyclones much more is known about the genesis of extratropical cyclones. However far from all is known, and there is still a lot of research to do in this area.

The deepening of an extratropical low in its generating stage is mostly due to conversion of the atmosphere's available potential energy to kinetic energy in the cyclone. This conversion of energy leads to a lowering of the centre of mass in the involved air mass. To achieve this phenomenon cold air must sink and warm air must rise on average in the three dimensional motion systems creating the cyclone. Release of latent heat by condensation through the rising of warm and moist air generally plays a significant role in the intensification of cyclogenesis. However, the process is not as crucial for the intensification as it is for the development of tropical cyclones.

The cyclogenesis of extratropical cyclones is a form of instability in the troposphere that is very dependent on positive feedback mechanisms involving diabatic and advective processes. Some of these processes are described more comprehensively than others in the text below. That is because they are believed to have played a more important role for Sandy in the transition from being a hurricane to an extratropical cyclone [Nielsen, 2003].

Differential Vorticity Advection

Differential vorticity advection is important for strengthening (or creating) an extratropical low. In the case study this phenomenon occurs when Sandy is transformed from being a hurricane to an extratropical low while interacting with an upper level trough.

A vorticity maximum is located at the through axis and a vorticity minimum is located at the ridge axis [Bluestein, 1993]. This can easily be shown (done by Holton, 2004) by considering the geostrophic vorticity; $\xi_g = \partial v_g/\partial x - \partial u_g/\partial y = \mathbf{k}\cdot\nabla \times \mathbf{V}_g$. Here v_g is the velocity component in the south-north direction and u_g the velocity component in the west-east direction and $\mathbf{V}_g$ is the geostrophic wind (in the quasi-geostrophic system). The geostrophic wind is defined as $\mathbf{V}_g \equiv f_0^{-1}\mathbf{k}\times\nabla\Phi$, where Φ represents the geopotential height and f_0 is the Coriolis parameter ($f_0 = 2\Omega\sin\phi_0$) with a reference latitude ϕ_0. The components in the geostrophic wind can be expressed as;

$$f_0 v_g = \frac{\partial\Phi}{\partial x}, \quad f_0 u_g = -\frac{\partial\Phi}{\partial y}. \tag{13}$$

Thus, the geostrophic vorticity can be expressed as;

$$\xi_g = \frac{\partial v_g}{\partial x} - \frac{\partial u_g}{\partial y} = \frac{1}{f_0}\left(\frac{\partial^2\Phi}{\partial x^2} + \frac{\partial^2\Phi}{\partial y^2}\right) = \frac{1}{f_0}\nabla^2\Phi. \tag{14}$$

Since the Laplacian, ∇^2, of a variable (in this case Φ) in general has the opposite sign of the variable itself, equation (14) states that there is a local maximum of geostrophic vorticity where there is a local minimum of Φ i.e. in the trough axis [Holton, 2004].

There is a positive (cyclonic) vorticity advection downstream a trough axis (downstream a vorticity maximum) and there is a negative (anticyclonic) vorticity advection downstream a ridge axis (downstream a vorticity minimum). This comes from the QG vorticity equation, see eq. (20).

Assume that there is a cyclone at lower levels situated to the east of the through axis (downstream the trough axis). Then cyclonic vorticity advection increases with height due to closed circulations of pressure (which has no vorticity advection) at the lower levels. When there is positive differential vorticity advection, then there is convergence at the surface and rising air which leads to a pressure fall [Bluestein, 1993]. This follows by the QG omega, ω, equation which can be written in the following way;

$$\left(\nabla_p{}^2 + \frac{f_0{}^2}{\sigma}\frac{\partial^2}{\partial p^2}\right)\omega = -\frac{f_0}{\sigma}\frac{\partial}{\partial p}\left(-\vec{V}_g\cdot\nabla_p(\xi_g + f)\right) - \frac{R}{\sigma p}\nabla_p{}^2\left(-\vec{V}_g\cdot\nabla_p T\right). \tag{15}$$

where ξ_g is the relative vorticity, f is the planetary vorticity and σ is the static stability parameter.

The omega equation describes vertical motion in the atmosphere and the derivation is described e.g. in Holton, 2004, section 6.2-6.4. In this version of the omega equation, for simplicity, diabatic heating and friction has been neglected. Further it has been assumed that the static stability parameter is a positive constant. To achieve a greater understanding of the omega equation it is better to simplify equation (15) even further so that it is easier to discuss the equation. This has been done in Nielsen, 2003.

The operator $\nabla_p{}^2 + f_0{}^2/\sigma\cdot\partial^2/\partial p^2$, is similar to the 3-dimensional Laplace operator. The Laplacian of a local minimum and maximum is in general positive and negative, respectively. Therefore (15) can be written (in a symbolic way) as:

$$\omega \propto \left(\frac{f_0}{\sigma}\mathrm{DVA}\right)_p - \frac{1}{\sigma}\mathrm{TA}, \tag{16}$$

where the vorticity advection is: $\mathrm{VA} = -\vec{V}_g \cdot \nabla_p(\xi_g + f)$ and the temperature advection is: $\mathrm{TA} = -\vec{V}_g \cdot \nabla_p(RT/p)$.

Since $\omega \propto -g\rho w$, where w is the vertical velocity then (16) can be rewritten as:

$$w \propto -\frac{f_0}{\sigma}(\mathrm{DVA})_p + \frac{1}{\sigma}\mathrm{TA} \tag{17}$$

Rewriting the first term on the right hand side in height coordinates instead of pressure coordinates yields;

$$w \propto \frac{f_0}{\sigma}(\mathrm{DVA})_z + \frac{1}{\sigma}\mathrm{TA}. \tag{18}$$

Interpretation of the above expression makes it clear that a positive differential vorticity advection gives rise to rising motion. Since there is positive vorticity advection downstream an upper level trough and that the low at the surface is a closed circulation there occurs positive differential vorticity advection in this area and thus rising motion [Nielsen, 2003].

It is easy to realize that if there is rising motion close to the surface; the pressure is going to decrease at the surface (even though there is convergence) since mass is moving away. For further conviction, done by Bluestein, 1993, one can derive the relationship between the local pressure tendency and local height tendency at ground level (which is done in the appendix *Derivations*), to yield:

$$\left(\frac{\partial p}{\partial t}\right)_{z=0} = \rho\left(\frac{\partial \Phi}{\partial t}\right)_p = \rho\chi_0. \tag{19}$$

This relationship states that if the local pressure surface at ground level falls, then the pressure at ground level also falls. Using equation (19) together with the frictionless form of the quasigeostrophic vorticity equation one can derive an expression for the geopotential height tendency at ground level. The frictionless Q.G vorticity equation can be written as:

$$\frac{\partial \xi_g}{\partial t} = -\boldsymbol{V}_g \cdot \boldsymbol{\nabla}_p\left(\xi_g + f\right) - \delta f_0. \tag{20}$$

where the relative vorticity on the left hand side can be replaced with $1/f_0\, \boldsymbol{\nabla}^2\Phi$ according to equation (14) and the divergence term, δ, can be replaced with $-\partial\omega/\partial p$ according to the equation of continuity. By doing so (and by assuming that $\omega = 0$ at the surface) one obtains the following expression;

$$\boldsymbol{\nabla}_p^2\frac{\partial \Phi}{\partial t} = \boldsymbol{\nabla}_p^2\chi_0 = f_0\left[-\boldsymbol{V}_g \cdot \boldsymbol{\nabla}_p(\xi_g + f)\right]_{p_0} + f_0^2\left(\frac{\omega_{p'}}{p_0 - p'}\right), \tag{21}$$

where $\omega_{p'}$ is the vertical velocity at the pressure level p' ($p' < p_0$) and $p_0$is the pressure at ground level.

Using equation (19) and (21) together it easy to infer that the pressure at ground level falls in areas where there is positive differential vorticity advection, convergence and upward motion [Bluestein, 1993].

Temperature Advection and frontal structure

One of the most characteristic features of an extratropical low is the frontal structure, which initially has a warm and a cold front. Since the cold front is faster than the warm front it will catch the warm front and the combination of them creates an occluded front. The fronts are connected to temperature advection; the warm front follows (by definition) the warm advection and the cold front leads (by definition) cold advection.

According to the omega equation, or the simplified version of it, see equation (18), warm advection $\left(\frac{1}{\sigma}TA > 0\right)$ leads to upward motion and thus to a pressure fall while cold advection leads to an increase of the pressure. In the idealized case (described below) the southerly wind component to the east of the pressure centre gives rise to that warm air is advected northward and the northerly wind component to the west of the pressure centre gives rise to cold air is advected southward [Bluestein, 1993].

2.3.2 The Life Cycle of an Extratropical Cyclone

The first theory about the life cycle of an extratropical cyclone was created by some famous Norwegian meteorologists (Bjerknes, Bergeron and Solberg) in Bergen at the end of World War I. The "Polar-Front theory" was based upon real surface observations and postulated that extratropical cyclones form along warm- and cold fronts at the surface. Nowadays this theory has many complementary theories and one of them postulates that cyclones at the surface often, but not always, intensifies when a lower level (e.g. the 850hPa level) region with strong horizontal (in this case a north-southward temperature gradient) temperature gradient associated with frontal zones, see *Figure 3,* gets superimposed by an upper level region with strong positive vorticity advection.[3] Such areas are normally found downstream an upper level trough which propagate in the eastward direction, see *Figure 4.*

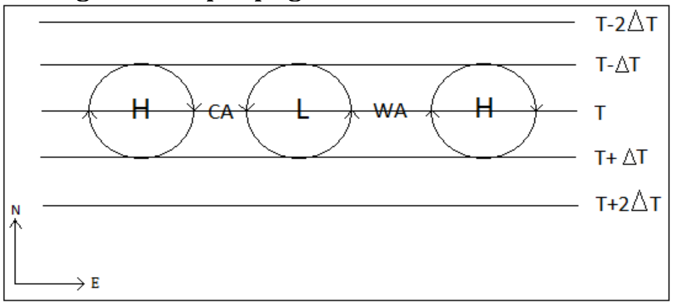

Figure 3 illustrates the idealized situation with a horizontal frontal zone at the lower levels in the atmosphere. In the frontal zone high- and low pressure systems are embedded with closed circulations. This gives rise to cold advection, CA, to the west/east of the low/high pressure systems and warm advection, WA, to the east/west of the low/high pressure systems.

Here an assumption is made that the upper level waves are sufficiently short so that the relative vorticity advection dominates over the planetary vorticity advection.

If the upper and lower regions (*Figure 3* and *4*) start to interact with each other and further if the low pressure regions tilt towards west with height then the surface cyclone will start to intensify. This is due to that there is going to be positive differential vorticity advection and warm advection above the surface cyclone and further to the east of it, which both induces upward motion and pressure fall. However this does not happen if the static stability is too strong.

[3] Extratropical cyclones may form and develop in different ways from the case described here. However, since this "idealized" case applies in one way or another to most developing extratropical cyclones it has been chosen to be demonstrated.

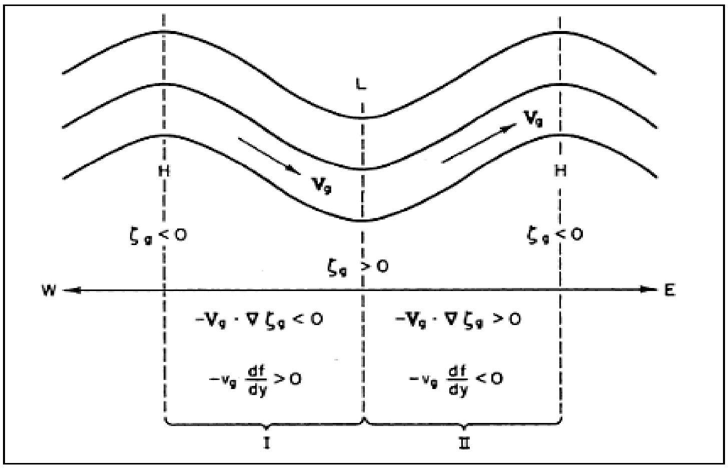

Figure 4 illustrates regions on an upper level (500hPa) sinusoidal wave with positive relative vorticity advection, downstream the trough and negative relative vorticity advection downstream the ridge. It further illustrates regions with positive and negative planetary advection. Courtesy to Holton, 2004.

Upward motion associated with cyclonic differential vorticity advection and warm advection to the east and northeast of the cyclone and corresponding downward motion to the west of the cyclone, associated with the cold advection give rise to energy conversion. Potential energy is converted into kinetic energy and the winds grow in strength. The opposite of cyclogenesis i.e. anticyclogenesis occurs to the west of the cyclone induced by cold advection and anticyclonic differential vorticity advection, which occurs downstream the upper level ridge.

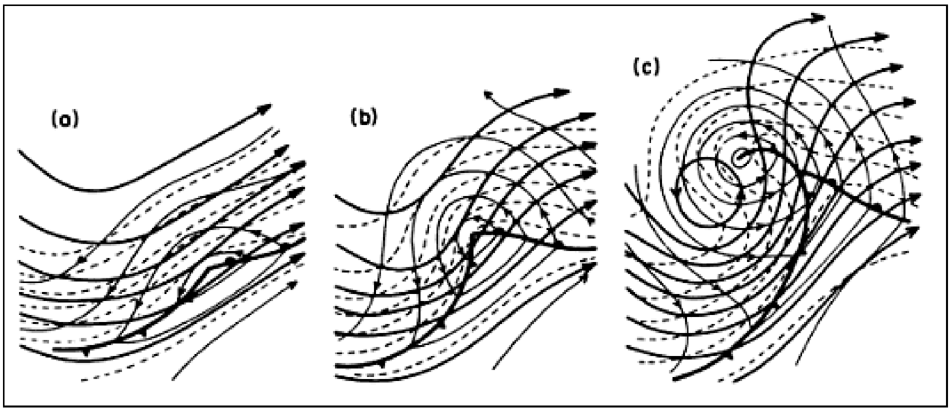

Figure 5 shows a schematic picture of the developing phase of a baroclinic low. The thin lines represent the contours at the 1000hPa surface, the solid lines the contours at 500hPa, whereas the dashed lines represent the thickness field between the 1000- and 500hPa surfaces. The warm front is caught by the cold front in an "earlier time" in this figure compared to the text. Courtesy to Holton, 2004.

As the cyclone advects cold air towards the equator and warm air towards the pole the isotherms become more and more meriodionally oriented (this is only valid if the local temperature change is mostly accomplished by temperature advection and not by the temperature changes owing to vertical motions). The cold advection that occurs underneath the trough axis leads to a deepening of the trough, see *Figure 5* (b) [Bluestein, 1993]. This comes from the geopotential tendency equation which can be expressed as;

$$\left(\nabla_p{}^2 + \frac{f_0{}^2}{\sigma}\frac{\partial^2}{\partial p^2}\right)\chi = -f_0\,\vec{V}_g\cdot\nabla_p(\xi_g + f) - \frac{f_0^2}{\sigma}\frac{\partial}{\partial p}\left(-\frac{R}{p}\vec{V}_g\cdot\nabla_p T\right). \tag{22}$$

where R is the gas constant for dry air. The geopotential tendency equation can be simplified in a similar manner as the omega equation which was done by Nielsen, 2003. The resulting approximate equation states the following;

$$\chi \propto -f_0 VA - \left(\frac{f_0^2}{\sigma}DTA\right)_z \tag{23}$$

At the trough axis the vorticity advection equals zero and under the trough axis the differential temperature advection increases with height which leads to that the geopotential height falls. Warm advection under the ridge axis leads to that the ridge amplifies (since $\chi = \partial\Phi/\partial t$) [Nielsen, 2003].

As time goes by, the warm advection leads to that warm air is advected more towards the north and poleward of the cyclone, while the cold advection causes cold air on the equatorward side of the cyclone, see *Figure 5* (b). Since a cyclone tends to move towards regions with warm advection and pressure fall and away from regions of cold advection and pressure rise, it starts to move more and more in the south-northward direction instead of in the west-eastward direction. Since the cyclone starts to move in this direction the cold front will start to move faster towards the east than the cyclone itself. Since the warm front moves towards north or even northwest it has a slower propagation speed than the cold front and the cold front will catch up with the warm front.

In the initial stage the upper level trough axis was situated to the west of the surface cyclone but since the surface cyclone gained a more south-northward track the upper level started to move faster towards the east than the surface cyclone. When the cold front catches up with the warm front the trough has become superimposed over the surface cyclone and the trough at upper levels tend to become closed circulations. The warm sector at lower levels is cut off from the cyclone and the system is said to be an occluded system, see *Figure 5* (c). Further the mechanisms for deepening of the cyclone have more or less vanished and the vorticity advection at higher levels has decreased a lot, which leads to that the movement of the upper level trough decreases. The movement of the system at lower levels also decreases due to the weakening of temperature advection. The system will continue to weaken until it eventually disappears [Bluestein, 1993].

2.4 ERA-Interim

ERA-Interim is the latest global reanalysis system at ECMWF and covers the period from January 1979 to near present and it is continuously extending forward in time [ECMWF, April, 2013]. ERA-Interim combines actual observations with a forecast model with the help of a data assimilation system and is thus able to create reanalysis. Far from all parameters available at ERA-Interim are actual observations but instead derived from different observed and interpolated fields. For instance it is possible to estimate the precipitation with the help of the reanalysis of wind, temperature and humidity.

All parameters available at ERA-Interim can be achieved in different resolution, depending on what kind of weather system examined [Dee *et al*, 2011]. All the values obtained from ERA-Interim represent a certain grid-point value. This grid-point value in turn represents the mean over a grid box [Andersson, 2011].

The advantages of using reanalyses compared to analyses (achieved from the operational forecasting system) are that the reanalysis provide spatially complete and coherent record of the evolution of the global atmosphere. They do so by only using one specific data assimilation system while the operational forecast system often changes method [Dee *et al*, 2011]. Due to the design and the resolution of reanalysis systems it is suitable to use the reanalysis for longer-term climate analyses (on larger scale) or for weather events that happened a long time ago. For extreme (short term) weather events that happened recently it is better to use (delayed cut-off) analysis produced from the high-resolution forecast system due to the higher resolution [Simmons *et al*, 2006].

2.4.1 Observations

The number of observations from all over the world which are assimilated into the reanalysis, has increased with a factor ten, to 10^7 observations per day, over the past two decades. Most of the increase is due to the extended use of satellites, which also is the instrument that contributes with the majority of the observations. Observations from satellites cover for instance ozone, atmospheric motion vectors from e.g. geostationary and polar orbiting sounders.

A minor, but still important, part of the observations e.g. of the 10m wind, surface pressure, the 2m relative humidity and 2m temperature, comes from the conventional observing system. This system includes observations from land stations, drifting buoys and ships. Further on it includes *in situ* measurements of upper levels parameters such as wind, temperature and specific humidity, obtained by wind profilers, aircraft and radiosondes.

All observations included in ERA-Interim undergo a quality control that consists of several steps so that many observations with errors are excluded. Errors that can occur are for instance errors while recording observations; like uncompleted reports, that parameters observed are not physically feasible and duplicate observations [Dee *et al*, 2011]. ERA-Interim almost uses all the observations that are used in operational forecast system at ECMWF. However they do not make use of all the available satellite observations for instance IASI data from MetOp are not used. This is due to that the current data assimilation system in ERA-Interim cannot handle this data at the moment and it requires a major upgrade of the system if one wants to use these additional observations [Dee *et al*, 2009].

When creating the reanalyses one uses the horizontal resolution T255 which corresponds to approximately 80x80km^2 and a vertical resolution that contains 60 levels where the top level is at the 0.1hPa surface [Dee *et al*, 2011].

2.4.2 The Forecast Model

The forecast model used in ERA-Interim is based upon the operational forecast, IFC (Integrated Forecast Model) Cy31r2 which was in operational use at ECMWF between December the 12th 2006 and June the 5th 2007 and which corresponds to a horizontal resolution of approximately 80x80km^2 [Dee *et al*, 2011].

For achieving consistency of the quality of the reanalysis it is important that the forecast model remains the same. For instance it could have been possible to replace IFC Cy31r2 with a better forecast model in order to achieve better reanalysis for the continuously generating reanalysis in near-real time. However since consistency of the quality of the reanalysis in ERA-Interim is important this has not been done [Dee *et al*, 2009].

2.4.3 The Data Assimilation system and 4-D Var

The reanalysis in ERA-Interim are created by combining prior information from the forecast model with available observations. The combination is done with the help of a sequential (intermittent) data assimilation scheme, see *Figure 6*, which advances forward in time in analysis cycles of 12 hours. To be able to do the estimate of the global atmosphere and its underlying surface one needs to do several different analyses; one needs to do separate analyses of near surface parameters such as the 2m temperature and humidity, ocean waves and snow. Further one needs to compute a variational analysis of the basic upper level fields such as wind, temperature, humidity and ozone. All these analyses are thereafter used to initialise a short-range model forecast, which in turn provides the next analysis cycle with the prior state estimates [Dee *et al*, 2011]. The most important component in the data assimilation system is 12 hourly 4D-Var which is the component that computes the variational analyses of the upper fields of e.g. temperature and winds. It creates a sequence of model states (reanalyses) within the analysis cycle that should be the closest fit between the forecast model and the observations [Andersson, 2011]. Additionally the 4D-Var system not just combines the forecast model with the available observations it further includes variational bias corrections for systematic errors in satellite data and observations.

The data assimilation systems which combine forecast model and actual observations have a smoothening effect on the obtained values [Dee *et al*, 2011].

The reanalysis system provides physical coherence between all the reanalysis i.e. that the parameters obey the law of physics as well as the observations. The change of one variable in the model generates changes in all other affected variables in order to maintain physical feasibility. Correction of e.g. the moisture field results in changes of the temperature and wind field as well [Andersson, 2011].

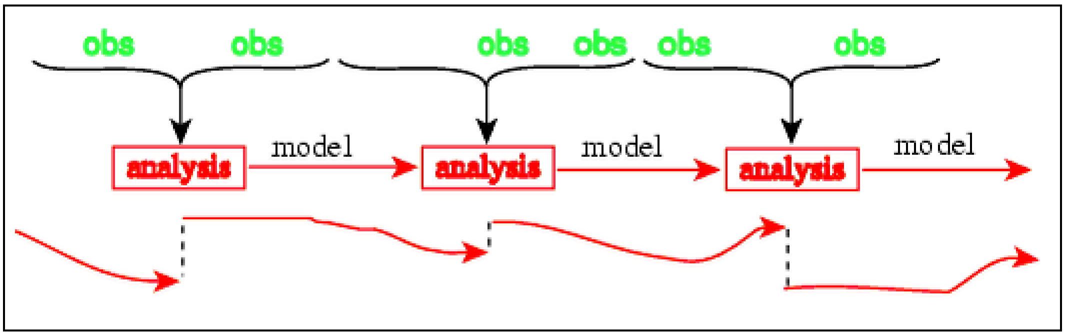

Figure 6 illustrates how a sequential intermittent data assimilation works. Courtesy to ECMWF. Source: [*http://www.ecmwf.int/newsevents/training/rcourse_notes/DATA_ASSIMILATION-/ASSIM_CONCEPTS/Assim_concepts2.html*](http://www.ecmwf.int/newsevents/training/rcourse_notes/DATA_ASSIMILATION/ASSIM_CONCEPTS/Assim_concepts2.html), 2013-06-10, time 12.54.

By making use of a forecast model and its governing equations it is possible to obtain values and information (in a physically meaningful way) about unobserved parameters by extrapolating information from locally observed parameters. It is also possible to carry this information forward in time, to the next analysis cycle. The better the forecast is (according to accuracy and skill) the greater the ability to retain the assimilated information and the less corrections are needed for maintaining consistency between the forecast and the observation as time goes by [Dee *et al*, 2011]. The forecast model is flow-dependent which means that the forecast may be more uncertain in a situation with deepening of tropical cyclones than in a situation with a subtropical high-pressure system [Andersson, 2011].

Further a wide variety of parameters are estimated by the model (which cannot be directly observed in a meaningful way) while producing the forecast, such as cloud properties, precipitation, turbulent fluxes etc. The quality and accuracy of these estimated parameters depend on how good the physics in the model is but also the quality of the analysis. Additionally those estimated parameters are constrained by all the available observations that are used for initialising the forecast [Dee *et al*, 2011].

2.4.4 Performance of ERA-Interim on an extreme weather event

ECMWF has investigated the performance of ERA-interim on a great (extratropical) storm, namely the Great Storm of October 1987 which affected both southern England and France. The short-term operational forecasts of that time failed to capture the storm's track, speed and intensity. A comparison between the (hand drawn) analysis from back then and plots achieved by ERA-Interim (with the model resolution T255) shows that the intensity and location deviates. The ERA-Interim plots show lower values of intensity. However, the intensity and location is much better represented by the ERA-Interim data compared to data from ERA-40 (the previous reanalysis system at ECMWF). Further the comparison shows that the storm moves a little too fast in the reanalysis (ERA-Interim). The comparison also shows that by increasing the forecast model resolution in ERA-Interim from T255 (0.75x0.75 of a degree grid) to T799 (0.22x022 of a degree grid), better results are obtained [Dee *et al,* 2011].

2.5 Forecasting Sandy

ECMWF and some other weather institutes showed greater skill forecasting Sandy compared to past similar weather systems. A comparison of operational forecasts from different centres (e.g. EMCMWF and NCEP), done by Magnusson *et al*, 2013, shows that ECMWF's operational forecast, HRES (high-resolution) together with ECMW's ENS (ensemble forecast) were the best ones forecasting the landfall of Sandy on the middle-range; 3-8 days. Up to 3 days before Sandy hit the east coast of the United States it was the NCEP (NOAA) forecast that showed the best results compared to the analysis.

Further Magnusson *et al*, 2013 made a comparison between five of their own forecasts models with very different resolutions; T_L3999 (5x5km^2), T_L1279 HRES forecast (16x16km^2), the control forecast used in ENS; T_L639, (32x32 km^2), T_L319 (64x64 km^2) and T_L159 (150x150 km^2). (The model forecast used in ERA-Interim has the same resolution as the resulting product, which approximately corresponds to 80x80 km^2 i.e. a somewhat lower resolution than for T_L319). In the experiment all the forecast models started out with the same analysis obtained from T_L1279 and the comparison has been made for 3- or 5-days forecasts.

The forecast models with higher resolutions show a greater accuracy in position and MSLP throughout the whole investigation than the forecast models with lower resolutions. Furthermore, the forecast models with lower resolution show a more eastward track before landfall (but in general they capture the track well), higher MSLP, a slower propagation mode and they do not capture the precipitation and the extremes in the wind as well as the ones with higher resolution [Magnusson *et al*, 2013].

3 Method

In this thesis it is investigated at what time Sandy truly was a hurricane (barotropic system), at what time it was a baroclinic system and at what time it was a combination of those two, a hybrid. Sandy was a weather system that developed in the Caribbean Sea, hit Cuba with hurricane force, lost some energy but progressed and regained force over the North Atlantic Ocean, before it eventually hit the United State; New Jersey as an extratropical cyclone in late October 2012. The results are presented in the *Case Study*. The main difference between a baroclinic (extratropical cyclone) and a barotropic (tropical cyclone) system is how they gain their energy. The former one gains it through baroclinic processes which arise from the temperature contrasts between cold and warm air masses and the latter one derives it from the release of latent heat through condensation in the eye wall. In a developing baroclinic system the system tilts with height [Blake *et al*, 2013] but in a barotropic system there is no or a little vertical tilting between the inflow of air at lower levels and the outflow of air at upper levels i.e. the low pressure system is approximately correlated with height [Kong and Elsner, 1998].

A variety of data sets, satellite images, additional observations, i.e. soundings etc. are available for investigating Sandy. It has been chosen to investigate how well the track, mean sea level pressure (MSLP), baroclinic respectively the barotropic structure etc. can be reconstructed by only public means.

To be able to do the case study, ERA-Interim Reanalysis (produced at ECMWF), are used as well as satellite images. That ECMWF's reanalysis system has been chosen over e.g. NCEP's reanalysis system is primarily due to that the parameters available at ERA-Interim fitted the purpose of the thesis. The reanalysis from ECMWF is a product of both actual observations and a forecast model, which both are included in a data assimilation system (see section 2.4 for a more comprehensive description of how the reanalysis are produced). The reanalysis is provided every sixth hour (00UTC, 06UTC, 12UTC and 18UTC) and the analysis of whether Sandy was a baroclinic or barotropic system is based on this sixth hour interval.

One could have included data from other institutes that also provided reanalysis data, but that has been chosen not to be done. This decision depends on the possibilities to evaluate how well the reanalysis from ECMWF coincides with the actual state of Sandy. The data of relevant parameters (e.g. MSLP, temperature at different pressure levels, vertical integral of kinetic energy), is downloaded as GRIB-files. The GRIB-files are decoded and then displayed in *GrADS* version 2.0.1. That *GrADS* has been chosen over e.g. Matlab is due to that *GrADS* is specially developed for working with and to display earth science data, including meteorological data. When having collected all the necessary data the analysis takes part. The analysis of the weather system is done with having all the theory presented in *Section 2* in mind. A "Best Track" of Sandy according to ERA-Interim is going to be made and presented in a table. A "Best Track" contains position, i.e. longitude and latitude, MSLP and maximum sustained winds at 6-hourly interval [NOAA/National Hurricane Center, 5th of May, 2013].

Generally one is interested in how strong the wind gusts are because those are the ones that bring most damage and are therefore included in the table. However, the wind gust cannot be achieved for one specific time. The data can be downloaded in 3, 6, 9 or 12 hours intervals from ECMWF but only at the time steps 00UTC and 12UTC. It was chosen to use the 12 hour interval data so that it covers the whole period of time, i.e. between 00-12UTC and 12-00UTC. The obtained value represents the wind gust (for the last 12 hours) with the greatest strength [Berrisford, 2009]. The table also contains if Sandy at time being experienced mostly baroclinic or barotropic features. It was chosen not to categorize (in the table) whether Sandy was a tropical cyclone or an extratropical cyclone etc. because according to the maximum sustained winds Sandy never reached hurricane force according to ERA-Interim, but the categorization is done in the *Case Study*.

To be able to do some kind of comparison of the values obtained from ERA-Interim and the real situation, a comparison of location (of the pressure centre), i.e. longitude and latitude, MSLP and wind speed will be made between the obtained values from ECMWF's ERA-Interim system and the best estimates from the *National Hurricane Center* (NHC), (that are assumed to be the closest fit to the real situation). This comparison is done so that an evaluation of the ERA-Interim can be made for this specific situation. The investigation cannot be compared with other weather phenomena that have occurred in the past, nor is it possible to draw any conclusion of how well the reanalysis performs in general since this thesis only investigates how well it performs on Sandy. The results of the best estimates from NHC are to be found in the appendix *Values and Data from the National Hurricane Center* or in the *Tropical Cyclone report- Hurricane Sandy* [Blake *et al*, 2013].

One of the greatest reasons that Sandy obtained the rare track that she did were due to the large-scale circulations that dominated the upper troposphere at that time. These circulations and their significance are discussed in the report *Evaluation of forecasts of Hurricane Sandy* [Magnusson *et al*, 2013] from ECMWF. In the above report a time series of analyses have been created comparing the geopotential height and the low pressure centre at ground level. Due to the importance of the upper levels large-scale circulation the same kind of charts have been produced (with the help of data from ERA-Interim) and in turn compared with the analyses from ECMWF. This is done for the possibility to evaluate the influence and importance of these circulations for Sandy in ERA-Interim. The comparison is presented under the section *Results.* Furthermore, I have been given the opportunity to do a small comparison of ERA-Interim data and high resolution delayed-cutoff analyses (which contains the same amount of observations as ERA-Interim) from ECMWF's operational forecast system. The comparison is done for MSLP, wind and total column of water vapor for some well-chosen time steps. That the total column of water vapor has been chosen to be investigated is due to that an eye is not apparent in the plots containing data from ERA-Interim. The aim of the comparison is to evaluate the importance of the resolution when creating forecasts, analysis and reanalysis.

The satellite images used in this thesis are obtained from Dundee Satellite Receiving Station, Dundee University, UK, from the satellite GOES East. At the times 00UTC and 06UTC images from the Channel 2 are used, which is a Mid-Infrared channel at wavelengths 3.8-4.0μm. At 12UTC and 18UTC, when there is sunlight present, a Visual-Green to Near-IR channel is used, Channel 1, which ranges between 0.5-0.7μm [NEODAAS, June, 2013]. Sunlight is not present at these time steps throughout the analysis and when not, Channel 2 is used. At the end of the *Case Study*, when Sandy has undergone the extratropical transition and thus has become an extratropical cyclone, fronts are drawn at the satellite images to illustrate this phenomenon. However, this is done without any other help than the clouds, which means that the fronts cannot be drawn correctly, e.g. it is impossible to find the correct point of occlusion without any other data.

I have created an external appendix which contains satellite images and the most important plots used for creating the *Case Study.* The sequence starts on October the 22nd, 00UTC and ends at October the 31th, 18UTC and it has a six hourly interval. The horizontal rows represent one time step and contain five different figures. The first one is a satellite image, the second one on the left hand side is a plot of geopotential height and temperature at the 800hPa pressure level, together with MSLP. The third plot contains MSLP, and the geopotential heights at the 800-, 500- and 200hPa surfaces, used as an indicator of whether the system experiences baroclinic or barotropic dynamics. The fourth plot is based on data of the 10m wind and the vertical integral of kinetic energy. The fifth and last plot in the row either contains the accumulated precipitation for the last twelve hours (00UTC and 12UTC) or the total column of water vapor (06UTC and 18UTC). That two different parameters are plotted are due to the availability of data.

Latent energy and latent heat

The latent heat release is the most important energy source for hurricanes and that fact is going to be used in the evaluation of when Sandy was a hurricane or an extratropical cyclone. The area with greatest evaporation rates, associated with hurricanes, occurs in the eyewall due to that the winds are found here [Emanuel, 2003]. Evaporation which is the phase change from liquid water into water vapor requires energy and heat. The opposite transformation, water vapor into liquid water releases energy and heat. From the theory section about tropical cyclones it is known that air in the eyewall is ascending and bringing water vapor to higher elevations with colder temperatures. At the *Lifting Condensation Level* (LCL), the air parcel becomes saturated with respect to a plane surface of pure water and the water vapor condenses back to liquid water creating the great cumulonimbus creating the eyewall [Wallace and Hobbs, 2006].

By plotting the vertical integral of latent energy, Lq, where L represents the latent heat and q the specific humidity one obtains a maximum in the area where most evaporation and condensation occur. At times when Sandy, as a hurricane, exhibited an eye there should be a maximum of vertical latent energy in the eyewall, surrounding the eye which has a corresponding minimum in latent energy.

Wind and Kinetic energy

Since the maximum winds in a hurricane are to be found close to the ground, the area with greatest magnitude of the 10m wind should coincide with the area of maximum value of the vertical integrated kinetic energy (while having a hurricane). This is going to be used as an indicator while deciding whether Sandy was a hurricane or not.

4 Results

The *Result* section starts with a *Case Study* which treats Sandy's behaviour and development using data from ECMWF´s reanalysis system ERA-Interim. The *Case Study* is followed by an evaluation of the upper level large-scale circulations effect on Sandy and a comparison of this, between analyses from ECMWF's high operational forecast system and reanalysis from ERA-Interim. Thereafter comparisons are made of MSLP and maximum sustained wind between the obtained values from ERA-Interim and the ones produced at NHC. The comparisons are showed in two different charts. The *Result* section ends with a table that contains location, minimum pressure and wind speed for every time step, a so called "Best Track" of Sandy, according to ERA-Interim. This table also contains whether Sandy mostly experienced barotropic or baroclinic features.

4.1 Case Study

According to Blake *et al*, 2013, Sandy can be traced back to the 11th of October 2012, at that point associated with a tropical wave leaving the west coast of Africa. The wave progressed towards west over the Atlantic Ocean with heavy showers and thunderstorms, but the vertical shear was too great for hurricane development. The track of Sandy, plotted by NHC is to found in the appendix *Values and Data from the National Hurricane Center.*

Investigation with the ERA-Interim data does not reveal this and I have chosen to start to analyse Sandy from 18UTC the 21th October. This time step has been chosen because that was the first time a closed low pressure system could be seen at the surface. The system was at this point of time localized over the southeastern Caribbean Sea. At this time step the system was of baroclinic nature since it was a low pressure system at lower levels whilst it changed to become a high pressure ridge at upper levels. By plotting the relative vorticity at 900hPa one could see a local maximum associated with Sandy with a value of $5 \cdot 10^{-5}\text{s}^{-1}$. Further the vertical wind shear was weak between the 900 and 500hPa pressure levels with a difference of only 0.5ms^{-1}. Between the 500hPa and the 200hPa pressure levels, it differed with somewhat more, 5ms^{-1}. The direction of the wind changed from being northeasterly, to north- northeasterly to once again become northeasterly at the three different pressure levels. This means that the vertical wind shear was weak at this time step which is one of the conditions that needs to be fulfilled for hurricane development. According to Blake *et al*, 2013 it was the interaction between the low pressure at lower levels and the high pressure system at upper levels that gave rise to an environment with a low vertical shear. Further the condition of that the sea surface temperature must exceed 26°C was also fulfilled.

The conditions of hurricane formation at this point were very favourable and a tropical depression developed.

As time progressed the winds strengthened while the pressure remained approximately the same and the above conditions were still satisfied. At 12UTC on the 22nd Sandy started to show tendencies for being a warm core structure at the 800hPa surface. However the temperature plot shows that the core is not correlated with the pressure centre; it is situated some degrees to the northwest of the centre. The temperature gradient is not especially great. The system started to show other features of being a hurricane e.g. that the magnitude of the wind started to decrease with height, e.g. between the 900 and the 500hPa levels it has decreased with, $1ms^{-1}$. Further the winds are weak in the centre and increases radially outward, but they do not reach a maximum in magnitude associated with the low pressure system which would have indicated that there would have been a tropical cyclone. Further, the geopotential lows at different pressure levels are not correlated with height and it tilts in the east-northeastward direction which indicates that the system still has a baroclinic nature. At higher levels there is still a high pressure ridge which strengthens the argument that the system still has a baroclinic nature.

The dynamics of the system remain similar to the ones described above for several time steps. The significant changes that occur are that; the systems start to "move away" from the upper level ridge while moving towards the northeast, that the clouds tends to be more and more axisymmetric around to the vortex axis (according to satellite images) and that the warm core structure seeks more and more towards the pressure centre.

At 12UTC the 24th Sandy is a well defined warm core system, located in the pressure centre at the 800hPa level. The strongest winds, approximately $27ms^{-1}$, are located southeast of the centre and additionally they decrease with height. At this time step NHC starts to refer Sandy as a hurricane. Additionally, the maximum values according to the vertical integral of kinetic energy coincide with the shaded area that represents the greatest magnitude in wind at the 10m height, which indicates that the system is a hurricane. However the data from ERA-Interim still shows a baroclinic structure of the system e.g. the low at the 500hPa surface is located approximately one degree to the southeast of the pressure centre at the surface. However, the conclusion drawn from above facts is that Sandy at this point exhibits more barotropic features than baroclinic.

At the next time step (18UTC) the winds close to the surface have decreased by approximately $10ms^{-1}$. This is very deviant from the NHC's best estimates, where the wind has increased with approximately $5ms^{-1}$. The reason for this is discussed in section 4.3 *Comparison of ECMWF's ERA- Interim and NHC's best track and estimates.* The main point is that Sandy, according to ERA-Interim feels a greater land area from Jamaica (due to resolution) and gets much more affected than what Sandy did in reality. An eye is for the first time apparent on the satellite image. This cannot be seen in the plot showing the vertical integral of latent energy.

At 00UTC the 25th October the mid-infrared satellite image shows a very pronounced eye. By plotting the total column of water vapor (TCWV) or the vertical integral of latent energy one should be able to see an eye, but this is not the case (however, by plotting the TCWV with data from the *"delayed cut-off analysis"* from ECMWF's high-resolution forecast system one obtains an eye, see section 4.2 *Comparison of different Data from ECMWF*). At this timestep the low is almost correlated with height (at least up to the 500hPa surface) but there is still some tilting above this level. There is a pronounced warm core structure but the 10m winds only show a maximum sustained value of $22ms^{-1}$. The system shows more of a barotropic structure than that of a baroclinic.

In the following time steps Sandy gets disrupted from its barotropic structure and once again the low is not correlated with height. For instance at 12UTC the 25^{th} the plot of MSLP and the geopotential heights at 800, 500 and 200hPa shows that neither the low at 800 or the one at 500hPa is correlated with the low at the surface but they tilt in different directions. This is probably caused when the system is moving over Cuba. Further the warm core system at the 800hPa level and the weakest winds (at 10 m height) are not correlated with their corresponding pressure centres anymore. According to all these facts I would say that Sandy mostly has baroclinic features but also some barotropic since there still is a warm core even though it is not correlated with the pressure centre. However, this was somewhat expected since Sandy just has moved over Jamaica and Cuba and since the power to the hurricane comes from the underlying warm water, the system has lost its engine. Losing this source is equivalent of losing its hurricane characteristics.

At the two previous time steps Sandy experienced a visible eye, but at 18UTC the 25^{th} the systems lost this characteristic. The warm core is not correlated with the pressure centre at lower levels and the same thing yields for the 500hPa level. Further neither the warm core nor the low are correlated with height. The system is still in contact with Jamaica and the winds over the island reach a magnitude of only $8\text{-}10ms^{-1}$. This implies that the system experiences more baroclinic than barotropic features at this time step.

For the next time step (00UTC the 26^{th}) the tendencies change a little bit. The low is now almost correlated in height and the warm core is almost correlated with the pressure centre. However no eye is shown in the satellite image. The maximum winds reach approximately $28ms^{-1}$ and the weakest winds are not exactly correlated with the pressure centre. At this time step the system experiences more barotropic features than baroclinic.

The two next time steps shows similar features as the previous ones but there and an eye is present at the satellite images for 12UTC the 26^{th}.

At 18UTC the 26^{th} there is an eye present on the satellite image, which is surrounded by a somewhat narrower eyewall to the southeast than to the north and west. This cannot be seen plotting the vertical integral of latent energy. On the satellite image one can also see a cold front approaching Sandy from the west. The temperature plots on the lower levels show a warm core structure where the core is more or less correlated with the pressure centre. However at the 500hPa level the warm core is not correlated with the geopotential low. The maximum winds are located northwest of the pressure centre and reach a magnitude of $26ms^{-1}$. The minimum wind speed is well correlated with the pressure centre. The plot showing the relationship between the low at the surface and the low at the pressure levels; 800, 500 and 400hPa looks more like an extratropical low in its deepening phase with a tilting of the system with height towards northwest. The vertical wind shear is no longer weak, which is one of the criteria that need to be fulfilled for a hurricane to survive. At this time step it is clear that the system exhibits more features of a baroclinic structure than that of a barotropic one.

From this time on Sandy starts to interact in a way with an upper level trough which causes the system to grow considerably in size and it continues to grow until the system finally dissipates. This can be seen in the satellite images found in the *External Appendix.* Additionally it is possible to see (in the plot showing the accumulated precipitation) that at time steps when Sandy experiences more baroclinic feature she also shows greater areas with precipitation.

The following two time steps show roughly the same structure and dynamics as the previous time step, exhibiting both baroclinic and barotropic features, but where the barotropic features dominates over the baroclinic. The tilting of the low with height gets weaker as time goes by, the maximum values of the vertical integral of kinetic energy coincide with the area of greatest wind magnitudes (at 10m height) and the wind decreases with height. The strongest winds are located to the left of the cyclone relative its movement which is not the general case for hurricanes. It is possible to see that Sandy induces a small scale ridge downstream the upper level trough. The induced small scale ridge probably prevented additional interaction of the upper level trough and Sandy.

However this phenomenon of inducing a small scale ridge downstream the trough disappears at 12UTC the 27th and Sandy starts to interact with the upper level trough, through their relative vorticities, see the appendix *Plots for the Case Study*. The plots in this appendix show the interaction of relative vorticity between the systems for the whole period. It is this interaction between Sandy and this upper level trough that causes Sandy to gain a more northwesterly track than a northeasterly. Another contributing factor for this movement is the high pressure ridge situated over the Atlantic Ocean (see section 4.2).

It does not look like there is an eye present at the satellite image, but it is hard to say due to the resolution. The maximum values of the vertical integral of kinetic energy do not coincide with the area of greatest wind magnitudes at 10m height. However, above the area of the strongest winds at the surface the wind actually decreases with height. But in some areas close to Sandy there is great vertical wind shear. Additionally the warm core is still located in the pressure centre at lower levels and the lows are more or less correlated with height. I would say that Sandy still experiences more barotropic features than baroclinic despite the interaction with the upper level trough.

At 18UTC the 27th the lows are once again correlated with height and the winds are decreasing with height. Sandy is embedded in a baroclinic environment with strong vertical wind shear but the system is not influenced by the baroclinic environment and will not undergo the extratropical transition yet. Sandy is still located over water that exceeds 26^{o}C and there is a pronounced warm core which is correlated with height. However, there is still interaction between Sandy and the upper level trough through relative vorticity, but Sandy experiences more barotropic features than baroclinic at this time step.

The barotropic features of the system remain intact for some time steps forward, but it is not possible to observe an eye in the centre of the storm at the satellite images. One possibility for this is the following; assume that there is positive (relative) vorticity advection downstream the upper level trough. It is the relative vorticity that is shown in the appendix *Plots for the Case Study* (since there is no reanalyses for the vorticity advection) but by considering the evolution of the relative vorticity at the 200hPa surface and the wind barbs, it looks like there is positive vorticity advection centred over Sandy's pressure centre. Since there is closed circulation below the area with positive vorticity advection that in turn would result in upward motion at the surface (due to positive differential vorticity advection). This was investigated by plotting the vertical velocity at several pressure levels which all yield the same result; subsidence. Thus the effect of positive differential vorticity advection was counteracted by other processes that were favourable for eye formation. Exactly why there was not an eye at these time steps are hard to say but there must have been clouds at some levels within the eye that prevented an eye to be shown at the satellite images.

At the satellite image from 18UTC the 28th one can once again observe an eye and temperature plots of lower levels show a warm core structure. The lows are correlated with height which indicating that the system is of barotropic nature. The plot of the 200hPa relative vorticity shows interaction between the upper level trough and Sandy. A plot showing sea surface temperature and MSLP for this time step shows a sea surface temperature associated with the pressure centre which is below 26°C. The following time step shows roughly the same features as the previous time step.

In the following time step, 00UTC the 29th, it is hard to decide whether there is an eye present or not due to the resolution of the satellite image; however, the cloud system rotates heavily around the storm axis. The warm core structure can be seen in several temperature plots, but it is more pronounced at the higher levels. The maximum winds reach $28ms^{-1}$. The low pressure system is correlated with height all the way up to the 400hPa surface. There is interaction of relative vorticity at the 200hPa surface and the sea surface temperature correlated with the pressure centre is still under 26°C. At this time step the system clearly exhibits both baroclinic and barotropic features where the barotropic features still dominates. The next time step shows approximately the same features.

At 12UTC the 29th is it hard to decide whether there is an eye present or not due to the resolution of the satellite image. However, the cloud system is very rotational around the storm axis close to the centre. Away from the centre it looks like there is frontal structure. Zoomed out plots of the temperature structure at the 800hPa surface show a somewhat protracted warm core around the pressure centre but also frontal structures with a warm sector. The lows and their pressure centres at different levels are still correlated with height but the geopotential height at the 500hPa surface almost shows a trough axis all the way in to the axis of the lows. It seems, compared to the previous and the next time steps, like the geopotential height at this surface acts the other way around the development in extratropical cyclones, where the trough tends to close of circulations with time. Here it seems like the closed circulations open up to "build" an upper level trough with time. However the winds are decreasing with height which is very characteristic for a barotropic system. At this time step one can see an interaction through the relative vorticity both at the 200 and the 500hPa pressure levels. The system clearly exhibits both baroclinic and barotropic features. According to above facts I would say that the extratropical transition occurs around this time step and I have chosen to classify Sandy as a hybrid.

From the 29th October 18UTC, the satellite images are not going to show any eyes. The surface low and the low at the 800hPa surface are still correlated while the low at the 500hPa has moved its pressure centre 0.5 degrees to the southwest compared to the former ones. The tendency of "building" a trough persists. At this time step one can see interaction through the relative vorticity both at the 200 and the 500hPa pressure level. The temperature structure of the 800hPa level shows that the system exhibits a warm core correlated with the pressure centre at the same time as the temperature structure acts as the system has frontal structure. The winds are actually decreasing between the 800hPa level and the 200hPa level in the area around the warm core, but they increase with height in the surroundings. This means that the inner core system experiences barotropic feature while the outer experiences baroclinic features. According to this I have drawn fronts that do not extend all the way into the pressure centre, which can be seen in the *External Appendix*. The winds with the greatest magnitudes at 10m height, $28ms^{-1}$ are correlated with the greatest temperature gradient, which is located south of the system. This area does not coincide with the greatest values of the vertical integral of kinetic energy. From the previous time step the pressure has fallen with approximately 9hPa and the system is intensifying. This is probably due to positive differential vorticity advection. According to Blake *et al*, 2013, this intensification was also due to that Sandy moved over the warmer water of the Gulf Stream. This is not apparent in plots showing the sea surface temperature with data from ERA-Interim. At this time step I have chosen to categorize Sandy as a hybrid due to barotropic inner core and the surrounding baroclinic environment. According to *Chart 1* Sandy made landfall in New Jersey late evening the 29th.

At 00UTC the 30th the temperature structure has changed a lot since the last time step. Temperature plots of the lower levels in the atmosphere still show a sign that it before was a warm core system, which is that the former warm core is embedded in the frontal structure with a slightly higher temperature than its surroundings, but it is not correlated with the pressure centre anymore. According to the reanalysis the warm sector is quite large. The pressure centres are not correlated with height but instead tilts with height to the south- southwest (but just slightly between the low at the surface and the geopotential height at the 800hPa surface). The system still experiences a barotropic inner core (winds decreasing with height) and baroclinic environments (winds strengthening with height). The greatest wind magnitudes reach 28ms^{-1} and are located to the east of the pressure centre, as well as the greatest temperature gradient. According to NHC Sandy is an extratropical system at this point, the extratropical transition occurred at 21UTC the 29th October. According to above facts I have chosen once again to classify Sandy as a hybrid and I have decided to draw a warm- respectively a cold front on the satellite image, which does not extend all the way to the pressure centre.

At the next time step the plots show a weather system with frontal structure and there are no longer any signs of the former warm core structure (and thus no barotropic features with winds that are decreasing with height). The system shows only baroclinic features and it has become an extratropical cyclone. The maximum wind speed has weakened to about 20ms^{-1}. A strong interaction through relative vorticity can be seen in both the plots at the 500hPa surface and the one at 200hPa. The pressure centre of the lows starts to organize in such a way that they more or less are correlated with height again (but this time due to occlusion). However, there is still a warm sector all the way in to the pressure centre even though it has weakened and that the temperature difference with the surroundings has become smaller since the previous time step. The geopotential low at the 200hPa surface is located to the southwest of the system.

MSLP has increased with approximately 14hPa since the previous time step and according to theory this means that the extratropical cyclone is in its dissipating stage. With the above facts and with the help of the satellite image I decided to draw an occlusion that splits up into a warm- respectively a cold front. However, it is kind of hard to decide at this point whether to interpret two separated fronts or an occlusion. If you only consider the satellite image and the fact that the low has been filled up with 14hPa in six hours, then it is clear that it should be an occlusion. Considering only the facts that there still exists a warm sector and that the pressure centres are not well correlated with height, then the system should be drawn with two separate fronts.

After this point of time Sandy continues to fill up and the lows get more and more correlated with height. The low at the surface tends to live its own life in the later stage of Sandy's lifetime and is not influenced by the circulation at higher levels. The geopotential heights at middle levels in the atmosphere seem to be influenced by the trough at higher levels. According to the satellite images Sandy gets incorporated in the westerlies and I have chosen that the time for dissipation is 18UTC on October 31th.

4.2 Comparison of different Data from ECMWF

Comparison of MSLP, 10 m Wind and Total Column of Water Vapor

A small comparison of position, MSLP and wind speed, see *Table 1,* and plots of the total column of water vapor (TCWV), see *Figure 7*, has been made between values and data from ERA-Interim and Analyses from ECMWF's operational forecast system. The greatest difference between the analyses and the reanalyses is the resolution, since it is not the analysis that the forecast starts from but the so called delayed-cutoff analysis which contains the same amount of observations as ERA-Interim. The analyses have a spatial resolution of 0.25x0.25 of a degree grid compared to ERA-Interim's resolution; 0.75x0.75 of a degree grid.

The comparison has been done for some well-chosen time steps that represent some of Sandy's most important transitions or stages. The first three time steps included in the comparison are 12 and 18UTC the 24th and 00UTC the 25th, describing the transition from a tropical storm to a hurricane but also the landfall over Jamaica. The two last time steps in the comparison 12 and 18UTC the 29th describe the transition from being a hurricane to an extratropical cyclone, the extratropical transition, hours from landfall in New Jersey. *Table 1* contains values of position, MSLP and maximum sustained winds. It is obvious that the analyses provide much better values of MSLP and maximum sustained winds than the reanalyses when comparing with the values from NHC, see appendix *Values and Data from the National Hurricane Center*. Additionally it seems like the analyses have been better to predict the extremes of maximum sustained wind and MSLP (once again compared to NHC) at the later time steps, when the weather system had a greater horizontal extent.

Date/Time (UTC)	Lat (N^o) (ERA-Int)	Lat (N^o) (Analysis)	Lon (W^o) (ERA-Int)	Lon (W^o) (Analysis)	MSLP(hPa) (ERA-Int)	MSLP (hPa) (Analysis)	Windspeed (ms^{-1}) (ERA-Int)	Wind speed (ms^{-1}) (Analysis)
2012-10-24/12	17.3	16.5	75.8	76.5	994.13	981.89	27.03	26.18
24/18	18.0	17.8	76.5	76.5	986.84	977.06	21.95	25.35
25/00	19.5	19.0	76.5	75.8	989.23	984.65	20.52	27.71
29/12	37.5	37.0	69.8	70.5	965.32	953.18	29.79	32.98
29/18	39.0	38.5	72.0	72.8	956.40	946.07	27.16	35.44

Table 1 contains position, MSLP and maximum sustained winds for the reanalyses and analyses.

Figure 7 shows a comparison of the TCWV between the reanalyses (to the left) and the analyses (to the right). These plots really show the importance of resolution. At the time step 00UTC the 25th the satellite image shows an eye, this is not at all apparent in the reanalysis plot of TCWV (which yields similar results as plots of the vertical integral of latent energy would have shown) from ERA-interim, but it is clearly represented in the analysis plot.

2012-10-24 12UTC

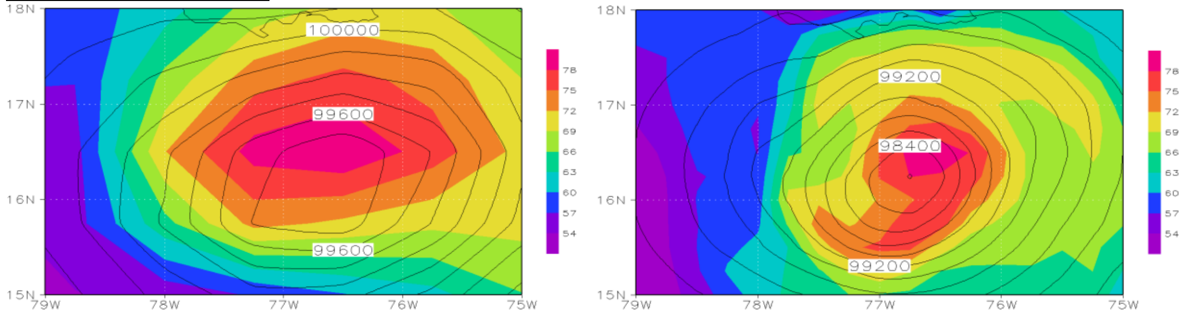

2012-10-24 18UTC

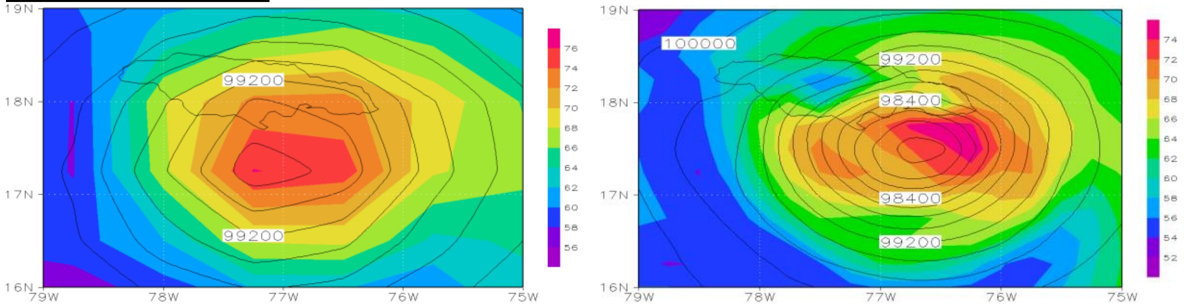

2012-10-25 00UTC

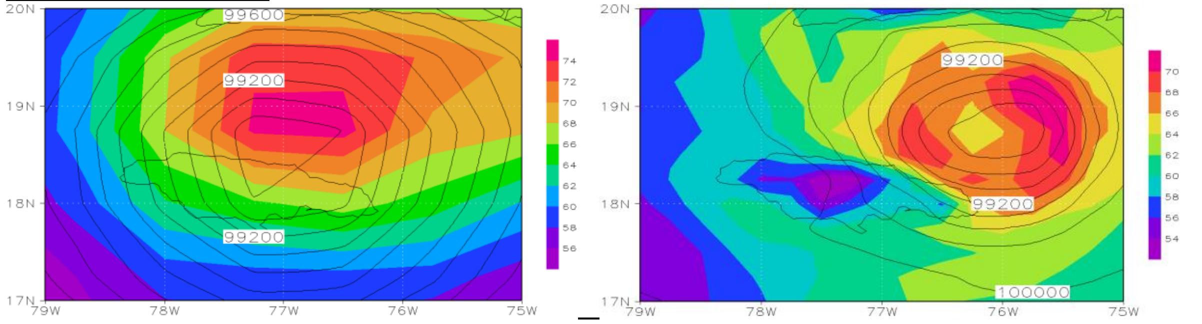

2012-10-29 12UTC

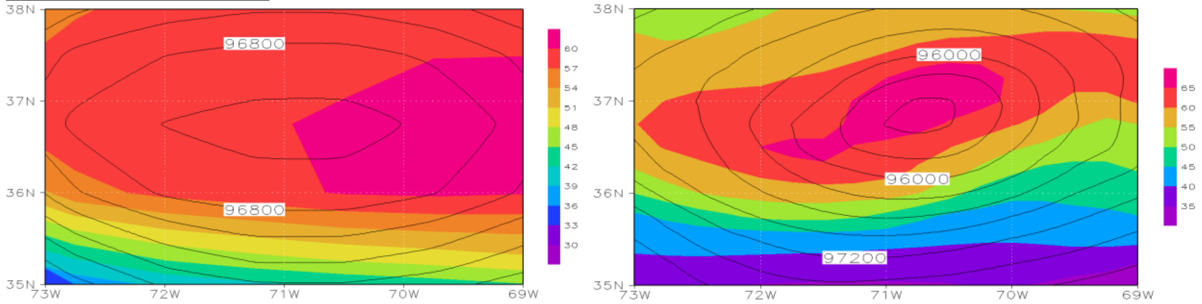

2012-10-29 18UTC

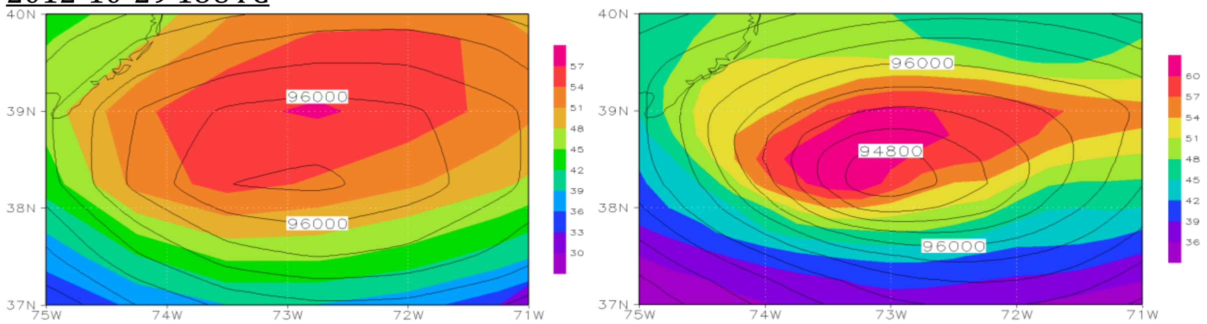

Figure 7 shows the differences in the total column of water vapor between reanalyses (to the left) and analyses (to the right) obtained from ECMWF.

The large-scale circulations affecting Sandy and a comparison between different resolutions

The prevailing large-scale circulations at the upper levels of the troposphere during the time period that Sandy acted, played a major role of how the system at the surface moved. The geopotential height on the 200hPa level has been chosen to demonstrate the influence of the circulation at the upper levels on the weather system close to the surface. However, the effect was especially prominent after Sandy had moved out from the tropics, which clearly can be seen in the plots where the system at the ground follows the isolines at the upper levels [Magnusson *et al*, 2013].

The interaction between upper and lower levels for 23-30 October, every 24 hours (00UTC), can be seen in *Figure 8*. The left panel shows analyses made by ECMWF and the right panel shows the reanalyses made with the help of GrADS with data from ERA-Interim. The plots range from the latitudes 10°-70°N and the longitudes 30° -160°W. The reason for having both analyses and reanalyses is for the possibility to compare the ERA-Interim plots with the analyses (a better estimate of reality due to resolution) and to evaluate whether they represent the upper level circulation in a useful way or not.

At the beginning Sandy moves towards north-east which is the most probable way of how hurricanes move in October (see *Figure 1*) in this area. However, after passing Jamaica and Bahamas Sandy starts to turn towards the north- northwest.

That Sandy does not move towards the northeast as hurricanes generally do is due to the fact that Sandy moves to the left of an amplifying ridge over the Atlantic. This amplification is primarily due to that the ridge is squeezed in between an eastward propagating trough to the west and a cut-off low to the east of it. Sometime between 00UTC the 26th and 00UTC the 27th Sandy starts to interact with the approaching upper level trough from the west (by e.g. interaction of relative vorticity). This was described in the case study above, but it can also be seen in *Figure 8.* This interaction is the primary reason Sandy starting to move against the US east coast at later time steps. However, this interaction also makes Sandy to reintensify before the landfall (after the extratropical transition) due to the positive feedback mechanisms of differential vorticity advection, which gives rise to a pressure fall close to the ground.

The overall tendencies in the upper-level circulation are the same when comparing the analyses and the reanalyses. The small differences in the large-scale upper level circulations between the analyses and reanalyses probably do not have an especially great impact on why the values of the analyses and reanalyses differed on smaller scale, e.g. MSLP and maximum sustained winds, see *Table 1*.

2012-10-23 00UTC

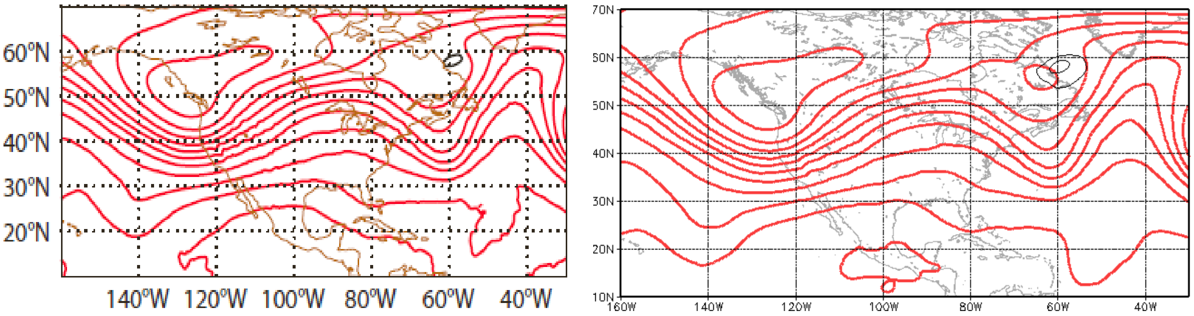

2012-10-24 00UTC

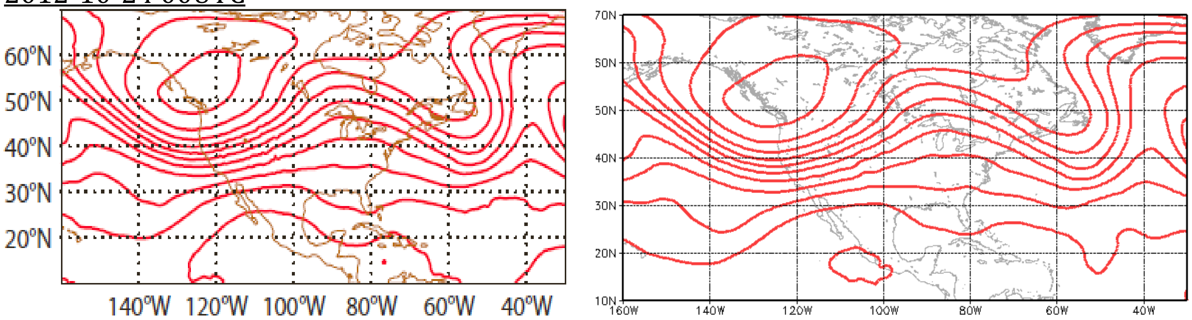

2012-10-25 00UTC

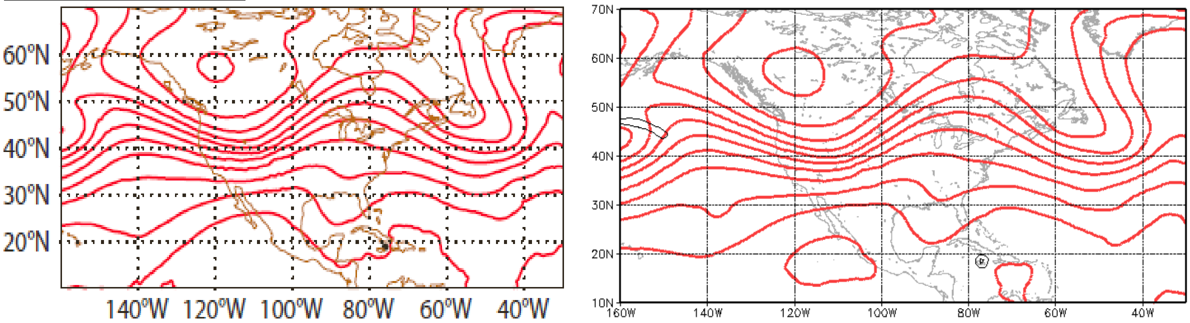

2012-10-26 00UTC

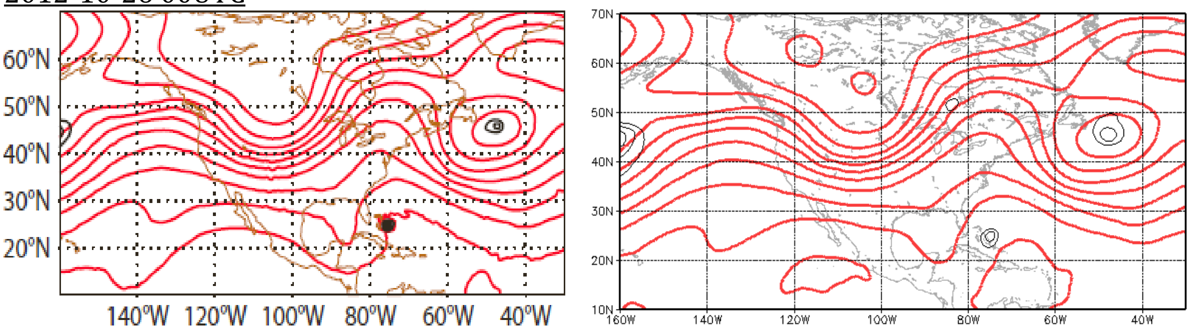

2012-10-27 00UTC

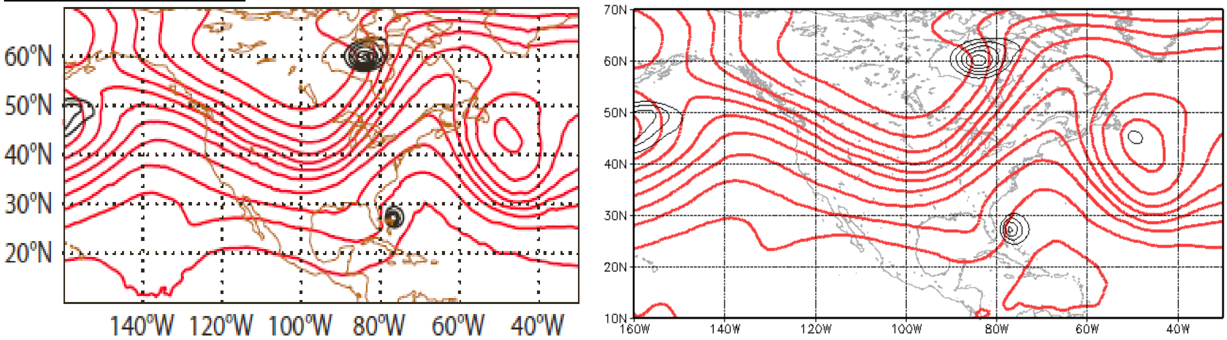

2012-10-28 00UTC

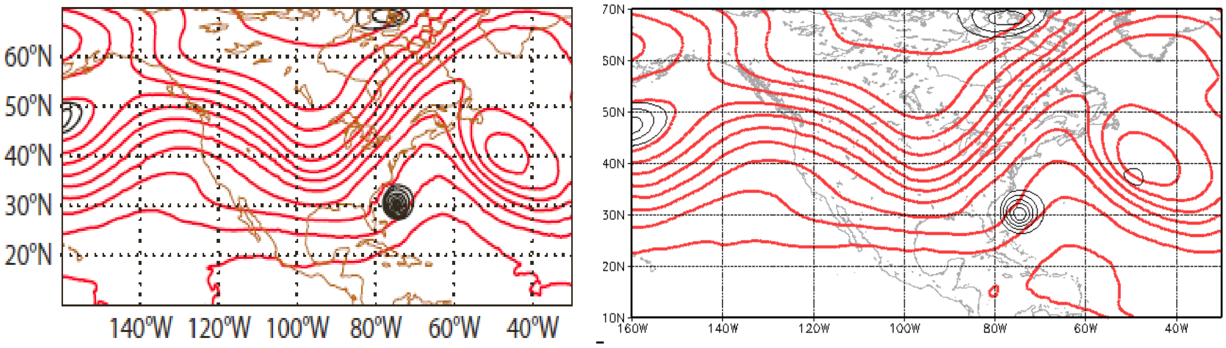

2012-10-29 00UTC

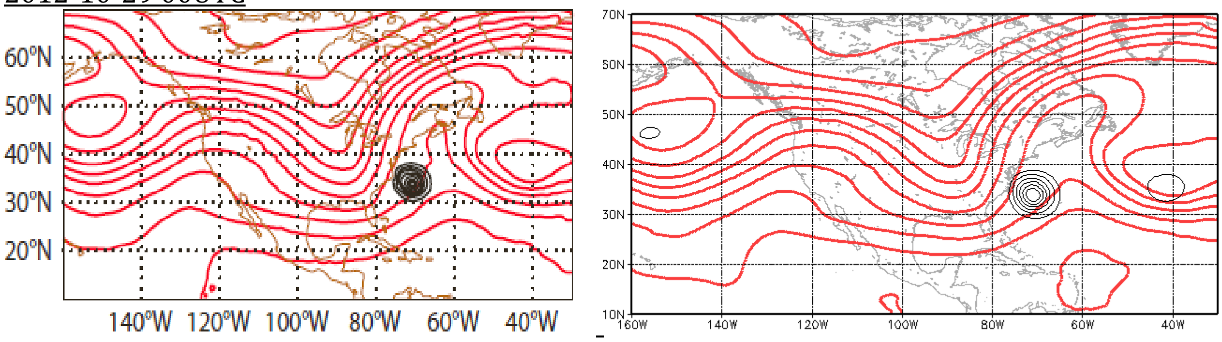

2012-10-30 00UTC

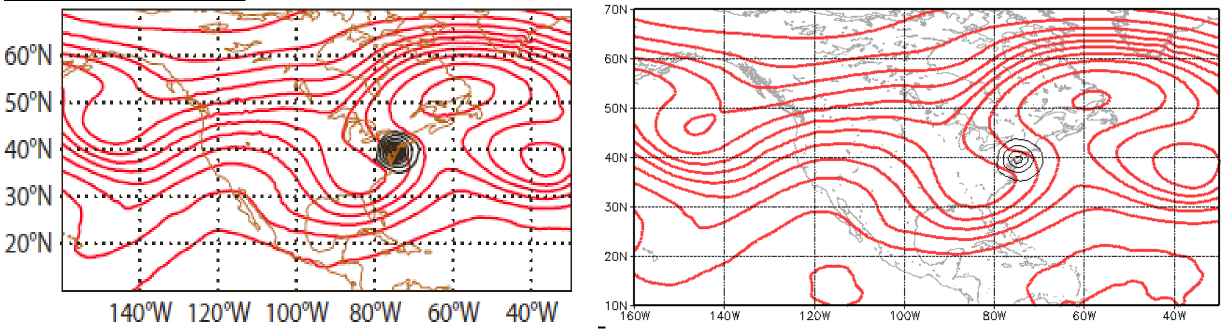

Figure 8 shows the geopotential height (red) at the 200hPa surface and MSLP(black). The left panel shows the analyses made by ECMWF and MSLP (below 990hPa) and the right panel shows the reanalyses from ERA-Interim with a lower resolution and MSLP (below 995hPa).

4.3 Comparison of ECMWF's ERA-Interim and NHC's best track and estimates

The best estimates according to ERA-Interim of position (longitude and latitude), MSLP, wind and wind gust are presented in *Table 2.* The best estimates of Sandy according to NHC can be found in the appendix *Values and data from the National Hurricane Center.* The values in these tables are used to create *Chart 1* and *Chart 2*.

Chart 1 shows a comparison of MSLP every six hours of Sandy's life time, between the ERA-Interim values (0.75x0.75 of a degree grid) and the NHC's best estimates. The overall tendencies of the pressure are coherent but the obtained minima are more or less deviant, where NHC's best estimates show much lower values than the one obtained from ERA-Interim. The first minimum (ERA-Interim; red line) in the chart represents the landfall of Sandy at Jamaica, approximately at 18 UTC the 24th, the other minima (NHC; blue line) represents when Sandy made landfall at Cuba which was 05.25UTC the 25th according to report *Tropical Cyclone Report- Hurricane Sandy*. According to the same report Sandy made landfall at Jamaica at late afternoon the 24th, i.e. approximately at the same time as the values from ERA-Interim shows. That the NHC data does not show a landfall at Jamaica might be due to the resolution. With higher resolution Jamaica is better represented while in lower resolution Jamaica becomes "larger" due to the representation of land in the grid boxes. This implies that Sandy, in reality, did not get so affected by Jamaica as she did according to ERA-Interim, which "experienced" a greater island. The two first minima obtained from NHC and ERA-Interim deviates by as much as 35hPa.

The two second minima in *Chart 1* (late evening the 29th) represent the point of time when Sandy made landfall in New Jersey. The minima are more or less equivalent in time but deviates with approximately 15hPa in pressure.

Chart 2 shows a comparison of estimated winds from NHC and ERA-Interim. The winds represent the maximum sustained winds. The first and last time steps follow the same tendencies but the two maxima apparent in the NHC data cannot be seen in the data from ERA-Interim. The two maxima in wind correspond to the two minima in MSLP which are apparent in *Chart 1*. The values representing ERA-Interim are lower than the ones representing NHC with a largest difference of approximately 40 knots (approximately 20ms^{-1}).

The wind gust values according to ERA-Interim represent the greatest wind gust for the last twelve hour period, from 00UTC to 12UTC or 12UTC to 00UTC and can be seen in *Table 1*. Wind gust is a measure over time which means that the values presented at every 00UTC and 12UTC step do not include the wind gust at that time step. This has to be clarified to avoid confusion since the wind gust at some time steps are lower than the maximum sustained wind presented at that time step. The winds gusts show really low values.

Due to the resolution of the reanalysis the position of Sandy according to MSLP does not get so good. The minimum pressure is always represented in a grid point which in turn represents the mean over a grid box. This means that Sandy's pressure centre needs to move great distances in the *x*- or *y*-direction to change to the next *x*-or *y*-coordinate within a time step. This was not always the case since sometimes several time steps in a row have the same *x*-and/or *y*- coordinate, see *Table 2*.

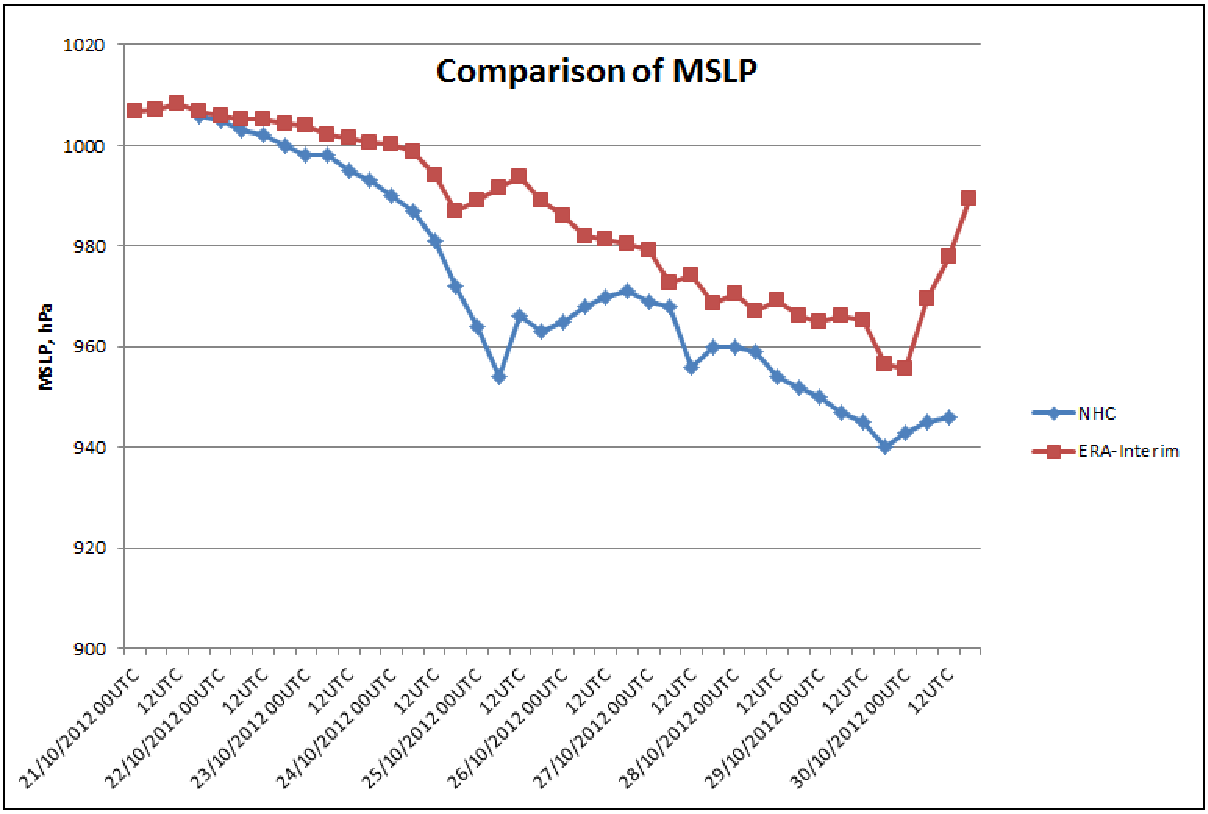

Chart 1 shows the differences in MSLP of Sandy between ERA-Interim (red line) and NHC (blue line).

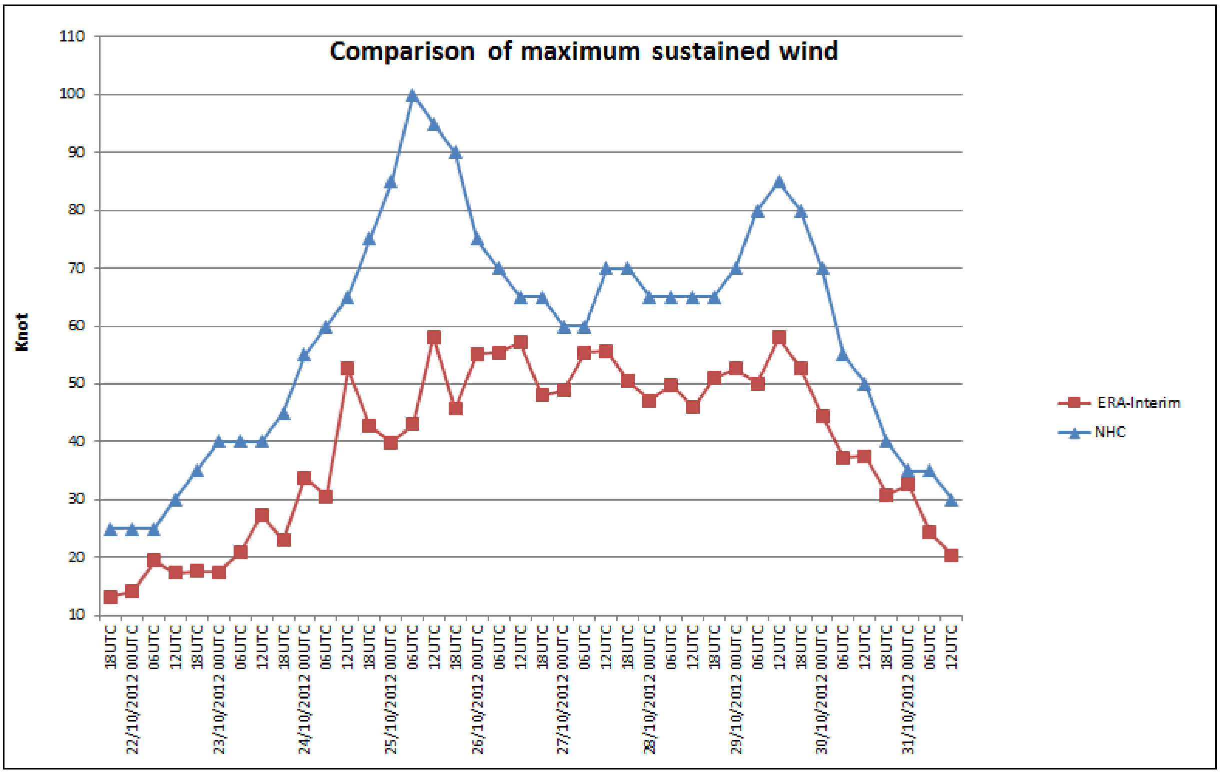

Chart 2 shows the differences in maximum sustained winds between ERA-Interim (red line) and NHC (blue line).

Date/Time (UTC)	Latitude (N°)	Longitude (W°)	MSLP (hPa)	Wind Speed (ms-1)	Wind Speed (kt)	Wind Gust (ms-1)	Wind Gust (kt)	Dynamics
2012-10-21/18UTC	14.3	75.0	1006.69	6.81	13.23	-	-	Baroclinic
22/00UTC	14.3	77.3	1005.99	7.27	14.13	9.45	18.37	Baroclinic
22/06UTC	13.5	78.0	1005.33	10.05	19.53	-	-	Baroclinic
22/12UTC	14.3	78.8	1005.16	8.94	17.38	11.09	21.56	Baroclinic
22/18UTC	13.5	78.8	1004.24	9.07	17.62	-	-	Baroclinic
23/00UTC	13.5	78.8	1003.95	9.01	17.5	13.73	26.69	Baroclinic
23/06UTC	13.5	78.8	1002.05	10.73	20.85	-	-	Baroclinic
23/12UTC	13.5	78.0	1001.60	14.08	27.38	13.48	26.20	Baroclinic
23/18UTC	14.3	78.0	1000.60	11.82	22.97	-	-	Baroclinic
24/00UTC	15.0	77.3	1000.12	17.35	33.72	15.76	30.63	Baroclinic
24/06UTC	15.8	75.8	998.87	15.71	30.53	-	-	Baroclinic
24/12UTC	17.3	75.8	994.13	27.03	52.55	22.91	44.53	Barotropic
24/18UTC	18.0	76.5	986.84	21.95	42.67	-	-	Barotropic
25/00UTC	19.5	76.5	989.23	20.52	39.89	27.81	54.06	Barotropic
25/06UTC	20.3	75.8	991.60	22.14	43.03	-	-	Baroclinic
25/12UTC	22.5	75.0	993.69	29.92	58.15	28.38	55.17	Baroclinic
25/18UTC	24.0	74.3	989.14	23.45	45.59	-	-	Baroclinic
26/00UTC	25.5	74.3	985.87	28.38	55.17	30.03	58.37	Barotropic
26/06UTC	26.3	75.0	981.99	28.49	55.39	-	-	Barotropic
26/12UTC	27.0	75.8	981.42	29.38	57.10	40.51	78.75	Barotropic
26/18UTC	27.8	75.8	980.33	24.72	48.06	-	-	Baroclinic
27/00UTC	27.8	76.5	979.30	25.17	48.92	41.15	79.99	Barotropic
27/06UTC	29.3	75.8	972.21	28.54	55.47	-	-	Barotropic
27/12UTC	29.3	75.8	974.17	28.62	55.63	34.71	67.47	Barotropic
27/18UTC	30.8	75.0	968.75	25.94	50.42	-	-	Barotropic
28/00UTC	30.8	73.5	970.60	24.25	47.14	35.87	69.73	Barotropic
28/06UTC	32.3	72.8	966.98	25.62	49.79	-	-	Barotropic
28/12UTC	33.0	72.0	969.28	23.65	45.97	32.08	62.36	Barotropic
28/18UTC	33.8	71.3	966.19	26.26	51.05	-	-	Barotropic
29/00UTC	34.5	70.5	964.95	27.04	52.57	34.53	67.12	Barotropic
29/06UTC	36.0	69.8	966.13	25.72	50	-	-	Barotropic
29/12UTC	37.5	69.8	965.32	29.79	57.91	37.79	73.46	Hybrid
29/18UTC	39.0	72.0	956.40	27.16	52.80	-	-	Hybrid
30/00UTC	40.5	74.3	955.74	22.87	44.45	35.25	68.52	Hybrid
30/06UTC	40.5	75.8	969.56	19.29	37.29	-	-	Baroclinic
30/12UTC	40.5	77.3	977.88	19.30	37.52	30.83	59.93	Baroclinic
30/18UTC	41.3	78.8	989.36	15.85	30.80	-	-	Baroclinic
31/00UTC	42.8	80.25	992.77	16.73	32.52	25.62	49.80	Baroclinic
31/06UTC	42.8	80.25	994.02	12.47	24.24	-	-	Baroclinic
31/12UTC	42.8	78.8	995.77	10.50	20.41	21.36	41.52	Baroclinic
31/18UTC								Dissipated

Table 2. The best estimates of longitude, latitude, MSLP, wind and wind gust according to ERA-Interim with the resolution 0.75x0.75.

5 Discussion

The primary intention with this thesis was to investigate when Sandy was a tropical-, extra-tropical system or something in between, a hybrid, with the help of ECMWF's ERA-Interim. It turned out to be really hard to do an accurate analysis since the reanalysis of e.g. pressure and the maximum sustained wind differed a lot compared with NHC's best estimates. See *Chart 1* and *2*. Here I have assumed that the best estimates according to NHC are more or less consistent with reality. This assumption is based upon the facts that they have used e.g. comprehensive techniques while calculating the maximum sustained winds. Further they have had access to data that are not public e.g. drop- sounds from military aircraft etc. and compared those values with observed values. This changed focus a bit, to both perform a case study for Sandy but also to try to investigate why the ERA-Interim data was so deviant from the best estimates of the situation.

The *Case Study* shows that it is possible to get an overview of Sandy in terms of whether it was a barotropic or a baroclinic system. The interaction between Sandy and the upper level trough was well captured. The position of Sandy differed somewhat from reality according to ERA-Interim. However, the system could not predict the wind extremes or the mean sea level pressure in a satisfying manner.

Depending on how to define a hurricane according to the maximum sustained wind averaged over 10 (or 1) minutes or whether the system experiences a barotropic nature yields different results for Sandy according to ERA-Interim. By only taking into account that the maximum sustained winds need to exceed $33ms^{-1}$ in order to be classified as a hurricane, the results show that Sandy never reached hurricane force. However, if one uses the definition of that Sandy was a hurricane when the system showed predominantly barotropic features, then Sandy was a hurricane during several time steps, according to the reanalysis data.

In *Chart 1* the two first minima correspond to Sandy making landfall at Jamaica (ERA-Interim) and at Cuba (NHC). That Sandy does not get so affected by Jamaica in reality (according to NHC) is probably due to Sandy feeling more land area in the world of ERA-Interim. It is a resolution problem. The pressure in the two different minima differs by as much as 35hPa. The reasons behind that the data deviates by as much as it does depend on several factors. The main reason is once again due to the spatial resolution of the used reanalyses, which is much lower than the one used in the NHC report. Additionally, ERA-Interim does not include all available observations from satellites. However the resolution of the reanalyses is one of the highest available, with free access from ECMWF. Section 2.5 dealing with forecasts with different resolution strengthens the argument that higher resolutions yield better result as well as section 4.2, *Comparison of different Data from ECMWF.*

Since the forecast model used to create the reanalysis has a resolution of approximately $80x80km^2$, the resolution of the forecast is relatively low. Comparing this resolution with those in the comparison (in Section 2.5), then it is the second lowest. Assuming that the same errors occur in this forecast (even though the forecast period is not the same) as in the ones with lower resolution in the comparison, then the forecast model predicts a somewhat more eastward track (before landfall in the U.S), with lower propagation speed, higher MSLP. Furthermore, it cannot predict the wind extremes and the precipitation pattern will look different compared to reality. However, the errors should not be as large for the forecast model since it operates on a much shorter period of time than the ones participating in the comparison. The distance between the forecast data and the observation probably increases which leads to smoothening of the obtained value achieved by assimilation, hence giving more deviating results.

Comparing the locations of the pressure centre (obtained by the reanalyses and the analyses) in *Figure 7* it is possible to see different locations. However, they do not differ in the way predicted by the arguments connected to the forecasts e.g. slower propagation speed. On the other hand it could be so that the forecast model differs in the same way as the others but that the data assimilation in ERA-Interim corrects for that. This leads to the conclusion that reanalyses from ERA-Interim do not differ in the same way as the forecast models with lower resolution. However, they all show lower values of MSLP and maximum sustained wind.

Let us return to *Figure 7*. Since the model resolution in the reanalyses is much lower than the one in the analyses the land distribution looks very different. The higher resolution the more grid boxes leads to better resolution of the coastline e.g. the coastline is better represented in the analysis system compared to the reanalysis system. The impact of Sandy feeling "more" land in the latter system probably leads to that Sandy experienced more surface drag which in turn results in weaker winds and additionally it probably lead to the great difference in location between the pressure centres in the plots from 18UTC the 24th and 00UTC the 25th.

At 00UTC it is possible to observe an eye in the high resolution analysis (of TCWV) but not in the reanalysis which is only an effect of differences in resolution. Since the radii of an eye typically range between 30-60km it is hard to achieve an eye if the resolution is too coarse. Say that the eye has a radius of 40km, the eye will be covered by several grid boxes in the analysis but by only one in the reanalysis. Due to smoothening effects within the grid box and that a grid point value represents the mean over a box leads the eye not being apparent in the reanalysis. This depends on that the eye is surrounded by the eyewall containing high values of water vapour.

Due to the smoothening effect of the data assimilation system, from combining a forecast with actual observations, the reanalysis system probably does not provide e.g. the highest observed wind gusts nor the lowest values of MSLP. This problem is experienced by all data assimilation systems and cannot be fixed since there always will be difference between forecasts and observed values. The future will probably provide higher resolution to the models and then in turn improve the short range forecasts in general, which would result in forecasts and the observations converging. If so that would mean that the reanalysis will get better in the future since the negative smoothening effect will get smaller. However, better data assimilation system is at the cost of computational power.

Due to the fact that the forecast model is flow dependent it was probably a bit uncertain in predicting the genesis of Sandy while becoming a hurricane. Therefore the data assimilation between the forecast model and the available observations will become greater than for a situation with e.g. a high pressure ridge. This will lead to a smoothening effect on the reanalyses. Generally, it is really hard to predict the track of a hurricane, but in Sandy's case it went quite well according to both ECMWF and NHC. One reason is probably Sandy's relatively great size and her interaction with the upper level trough in the later stage of her life cycle.

The fronts drawn at the satellite images (included in the *External Appendix*) are done with no aid from other data or observations except from the clouds present at the image. This means that the fronts cannot be correctly drawn. It is e.g. impossible to find the correct position of where the occlusion starts. However, it has been chosen to be done to illustrate that there were fronts present at these time steps, but they are not supposed to be taken too seriously.

All the satellite images are taken from Dundee Satellite Receiving Station, Dundee University, UK, from the satellite GOES East. The images are not suitable for research due to the relatively coarse resolution. At some time steps it was really hard to decide whether there was an eye present in Sandy or not. Since the satellite images were part of making the *Case Study* it would have been better to have images with better resolution to be able to do a more accurate analysis. Satellite images with better resolution could not be found with public access.

6 Conclusions

- At time being it is possible to get an overview over past behaviour of mesoscale/ synoptic scale weather systems. However the smaller scale the system got the harder it is to get the overview due to resolution and the forecast model used in the reanalysis system.

- Wanting a good estimate of past mesoscale weather systems with the help of reanalysis, the system needs a higher resolution than the one available today. I would say that the resolution needs to get down to 0.1x0.1 of a degree grid. This assumption is validated since Sandy, according to NHC's best estimates, only moved 0.1 degree on a time period of six hours. Without this high resolution this cannot be captured.

- To do more accurate and detailed Case Studies (at time being) for extreme weather events that occurred not that long ago it is more appropriate to use delayed cut-off analysis from high resolution forecast systems. They provide a much higher resolution and they contain as much observations as the reanalyses does.

7 Acknowledgments

I would like to thank

Aksel Walløe Hansen, NBI for his ideas and support while writing this thesis,
Mattias Lind for all help with GrADS and all inspiration through the whole process,
Dick Dee, ECMWF for helping me to achieve a greater knowledge about ERA-Interim
and Linus Magnusson, ECMWF for his help with handing me additional ECMWF data, i.e.
high-resolution delayed cut-off analyses from ECMWF's operational forecast system.

8 Literature Cited

Bister M, Emanuel KA. 1998. Dissipative heating and hurricane intensity. *Meteorol. Atmos. Phys.* 50:233–40

Berrisford P, Dee D, Fielding K, Fuentes K, Kållberg P, Kobayashi S, Uppala S. 2009. The ERA-Interim archive, Version 1. ECMWF; *ERA Report Series*, number 1.

Blake, E., S., Kimberlain, T., B., Berg, R., J., Cangialosi, J., P., Beven II, J., L. 2013. Tropical Cyclone Report- Hurricane Sandy. Avail able: http://www.nhc.noaa.gov/data/tcr/AL182012_Sandy.pdf. Last accessed 7th of March, 2013.

Bluestein HB. 1993. The Formation of Surface pressure systems. In: *Synoptic-Dynamic Meteorology in Midlatitudes, Vol ume II, Observations and Theory of Weather Systems*, pp. 3-8. Oxford University Press, New York.

Dee DP , Berrisford P, Poli P, Fuentes M. Spring 2009. ERA-Interim for Climate monitoring. *ECMWF Newsletter No. 119.* 5-6.

Dee DP, Uppala SM, Simmons AJ, Berrisford P, Poli P, Kobayashi S, Andrae U, Balmaseda MA, Balsamo G, Bauer P, Bechtold P, Bel - jaars ACM, van de Berg L, Bidlot J, Bormann N, Delsol C, Dragani R, Fuentes M, Geer AJ, Haimberger L, Healy SB, Hersbach H, Hólm EV, Isaksen L, Kållberg P, Köhler M, Matricardi M, McNally AP, Monge-Sanz BM, Morcrette J-J, Park B-K, Peubey C, de Rosnay P, Tavolato C, Thépaut J-N, Vitart F. 2011. The ERA-Interim reanalysis: configuration and performance of the data assimilation system. *Q. J. R. Meteorol. Soc.* **137**: 553–597. DOI:10.1002/qj.828

ECMWF. http://www.ecmwf.int/research/era/dday/. Last accessed 6th of May, 2013

ECMWF. http://www.ecmwf.int/research/era-/do/get/era-interim. Last accessed 19th of April, 2013.

Emanuel K. 2006. Hurricanes: Tempests in a greenhouse. *Phys. Today 59(8), 74-75*; doi: 10.1063/1.2349743

Emanuel K. 2003. Tropical Cyclones. Annu. *Rev. Earth Planet. Sci. 31:75–104*; doi: 10.1146/annurev.earth.31.100901.141259

Holton JR. 2004 Mesoscale Circulations: Hurricanes. In: *An Introduction to Dynamic Meteorology, fourth edition*, ed. Cynar, F, Burlington, MA: Elsevier Academic Press.

Jones, Sarah C., and Coauthors, 2003: The Extra tropical Transition of Tropical Cyclones: Forecast Challenges, Current Understanding, and Future Directions. *Wea. Forecasting*, **18**, 1052–1092.
doi: http://dx.doi.org/10.1175/1520-0434(2003)018<1052:TETOTC>2.0.CO;2

Magnusson, L., Thorpe, A., Bonavita, M., Lang, S., McNally, T., Wedi, Nils. 2013. Evaluation of Forecasts for Hurricane Sandy. *Technical Memorandum No. 699.* Used with permission from ECMWF.

MetEd .http://www.meted.ucar.edu/Hurrican-/strike/text/htc_ttoc.htm. Published 24th of August 2010.

MetEd. http://www.meted.ucar.edu/hurrican-/chp/navmenu.php?tab=2&page=4.5.0. Last accessed 23rd of May, 2013

NASA. https://www.grc.nasa.gov/WWW/k--12/airplane/enthalpy.html. Last updated 11th of July, 2008.

Nielsen NW. 2003. Quasigeostrophic Interpretation of Extratropical Cyclogenesis. Danish Meteorological Institute, Scientific Report, 03-11.

NOAA/National Hurricane Center. http://www.srh.noaa.gov/jetstream/-tropics/tc_atlclimo_pct.htm. Last updated 5th of January, 2010.

NOAA/National Hurricane Center. http://www.aoml.noaa.gov/hrd/tcfaq/A11-.html. Last updated 20th of May, 2011.

NOAA/National Hurricane Center. http://www.nhc.noaa.gov/aboutsshws.php Last accessed 15th of April, 2013.

NOAA/National Hurricane Center. http://hurricanes.noaa.gov/pdf/hurricanebook.pdf. Last accessed 4th of May, 2013.

NOAA/National Hurricane Center. http://www.aoml.noaa.gov/hrd/tcfaq-/A15.html. Last accessed 23rd of May, 2013.

NOAA/National Hurricane Center. http://nhc.noaa.gov/aboutgloss/shtml. Last accessed 25th of May, 2013.

Kong, K and Elsner, J. B. 1998. *A note on the baroclinic structure of Hurricane Danny at landfall.* Technical Attachment. Available at: http://www.srh.noaa.gov/topics/attach/html/ssd99-19.htm. Last accessed 12th of June 2013.

NEODAAS, http://www.sat.dundee.ac.uk/geobrowse/geobrowse.php?sat=4. Last accessed 12th of June 2013.

Persson A. 2011. *User Guide to ECMWF forecast Products.* Available : http://www.ecmwf.int/products/-forecasts/guide/user_guide.pdf. Last accessed 9th of April 2013.

Smith, R. K., 1980: Tropical Cyclone Eye Dynamics. *J. Atmos. Sci.*, **37**, 1227–1232. doi: http://dx.doi.org/10.1175/1520-0469(1980)037<1227:TCED>2.0.CO;2

Simmons AJ, Uppala SM, Dee DP, Kobayashi S. Winter 2006/07. ERA-Interim: New ECMWF reanalysis product from 1989 onwards. *ECMWF Newsletter No. 110,* 25-35.

Wallace JM., Hobbs, P. 2006.*Atmospheric Science, An Introduction Survey,* Second edition, ed. Helé J. Burlington, MA: Elsevier Academic Press.

Appendices

Derivations

Derivation of the absolute angular momentum form of the gradient wind balance, for an axisymmetric hurricane.

The derivation starts out with the tangential velocity form of the gradient wind balance, eq. (9);

$$\frac{v_\lambda^2}{r} + f v_\lambda = \frac{\partial \Phi}{\partial r},$$

the absolute angular momentum and the tangential velocity is interrelated by $M_\lambda \equiv v_\lambda r + f r^2/2$. v_λ can thus be expressed in the following way;

$$v_\lambda = \frac{M_\lambda}{r} - \frac{fr}{2}.$$

Substitution gives the following;

$$\frac{v_\lambda^2}{r} = \frac{1}{r} \cdot \left(\frac{M_\lambda}{r} - \frac{fr}{2}\right) \cdot \left(\frac{M_\lambda}{r} - \frac{fr}{2}\right) = \frac{M_\lambda^2}{r^3} - \frac{M_\lambda f}{2r} - \frac{M_\lambda f}{2r} + \frac{f^2 r^2}{4r} = \frac{M_\lambda^2}{r^3} - \frac{M_\lambda f}{r} + \frac{f^2 r}{4}.$$

$$f v_\lambda = \frac{f M_\lambda}{r} - \frac{f^2 r}{2}.$$

Thus;

$$\frac{v_\lambda^2}{r} + f v_\lambda = \frac{M_\lambda^2}{r^3} - \frac{M_\lambda f}{r} + \frac{f^2 r}{4} + \frac{f M_\lambda}{r} - \frac{f^2 r}{2} = \frac{M_\lambda^2}{r^3} + \frac{f^2 r}{4} - \frac{2 f^2 r}{4} = \frac{M_\lambda^2}{r^3} - \frac{f^2 r}{4} = \frac{\partial \Phi}{\partial r}.$$

Derivation of the relationship between the local height and pressure tendency [Bluestein, 1993].

The purpose of this derivation is to show that if a pressure levels falls (that initially was at the Earth's surface) then the pressure at ground level also falls.

From the text we had rising motion above a levels surface which gives convergence;

$$\partial \omega / \partial p = -\delta > 0,$$

at the surface. This convergence at the surface leads to that the vorticity increases locally (makes it more cyclonic) according to the Q.G vorticity equation since;

$$\frac{\partial \xi_g}{\partial t} = -\delta f_0 > 0.$$

In the above expression the effects of friction and vorticity advection is neglected, since the only interesting term is the one expressing convergence. The vorticity can be expressed in the following way; $\xi_g = (1/f_0) \nabla_p^2 \Phi$. Replacing the vorticity with this expression in the above equation yields;

$$\frac{\partial}{\partial t}\nabla_p^2\Phi = \nabla_p^2\left(\frac{\partial\Phi}{\partial t}\right) > 0.$$

Since the Laplacian of a local maximum tends to be negative, this means that the height tendency is negative, while having rising motion.

Now it is time to derive the relationship between the local height- and pressure tendency. We start to consider the total differential of pressure as a function of *x, y, z* and *t.*

$$dp = \left(\frac{\partial p}{\partial x}\right)dx + \left(\frac{\partial p}{\partial y}\right)dy + \left(\frac{\partial p}{\partial z}\right)dz + \left(\frac{\partial p}{\partial t}\right)dt.$$

The third term on the right hand side is rewritten with the help of the hydrostatic equation to achieve an expression that contains the geopotential height; $(\partial p/\partial z)dz = -g\rho dz = -\rho d\Phi$ which leads to;

$$d\Phi = -\frac{1}{\rho}dp + \frac{1}{\rho}\left(\frac{\partial p}{\partial x}\right)dx + \frac{1}{\rho}\left(\frac{\partial p}{\partial y}\right)dy + \frac{1}{\rho}\left(\frac{\partial p}{\partial t}\right)dt.$$

Now we instead consider the total differential of the geopotential height as a function of *x, y, z* and *t;*

$$d\Phi = \left(\frac{\partial\Phi}{\partial x}\right)dx + \left(\frac{\partial\Phi}{\partial y}\right)dy + \left(\frac{\partial\Phi}{\partial p}\right)dp + \left(\frac{\partial\Phi}{\partial t}\right)dt,$$

where the right term on the right hand side can be rewritten as: $(\partial\Phi/\partial p)dp = (\partial/\partial p \cdot gz)dp = (\partial z/\partial p \cdot g)dp = (g \cdot 1/-g \cdot \rho)dp = -\,dp/\rho$ which leads to;

$$d\Phi = -\frac{1}{\rho}dp + \left(\frac{\partial\Phi}{\partial x}\right)dx + \left(\frac{\partial\Phi}{\partial y}\right)dy + \left(\frac{\partial\Phi}{\partial t}\right)dt.$$

Further we have that;

$$-\frac{1}{\rho}\left(\frac{\partial p}{\partial x}\right)_z = -\left(\frac{\partial\Phi}{\partial x}\right)_p$$

$$-\frac{1}{\rho}\left(\frac{\partial p}{\partial y}\right)_z = -\left(\frac{\partial\Phi}{\partial y}\right)_p,$$

which means that some terms in eq. 2 and 4 cancels each other out and leaves us with the following expression;

$$\frac{1}{\rho}\left(\frac{\partial p}{\partial t}\right)_z = \left(\frac{\partial\Phi}{\partial t}\right)_p,$$

which states that if the height of the pressure surface that is located at ground level falls, then the pressure (at the same level) also falls.

Plots for the Case Study

2012-10-26 12UTC

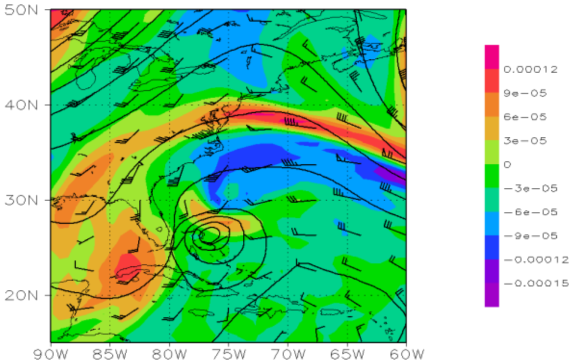

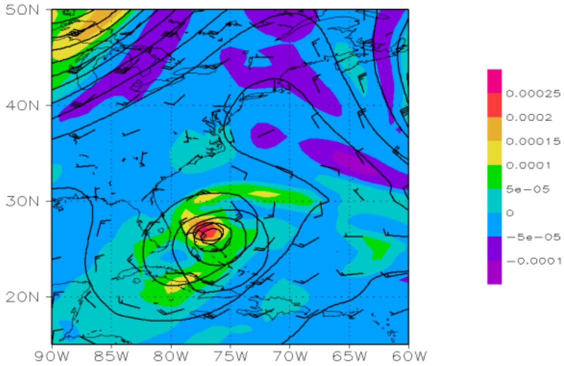

2012-10-26 18UTC

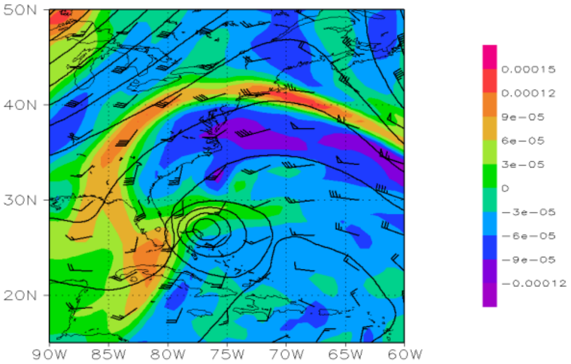

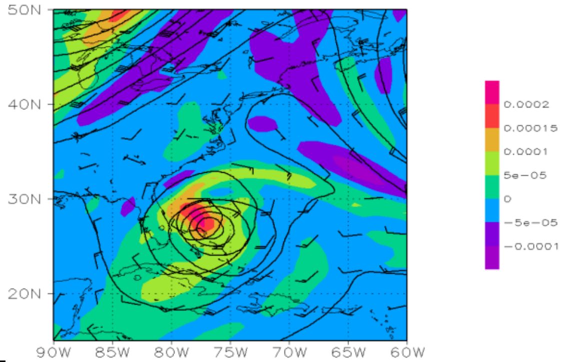

2012-10-27 00UTC

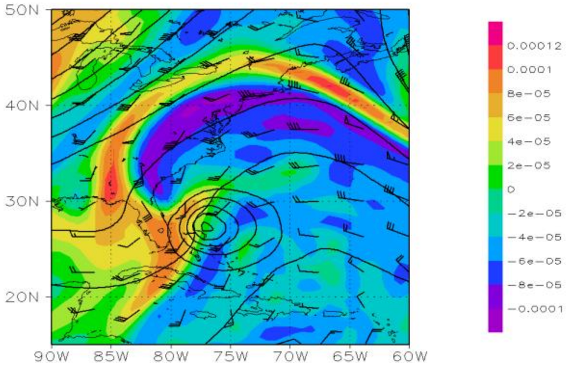

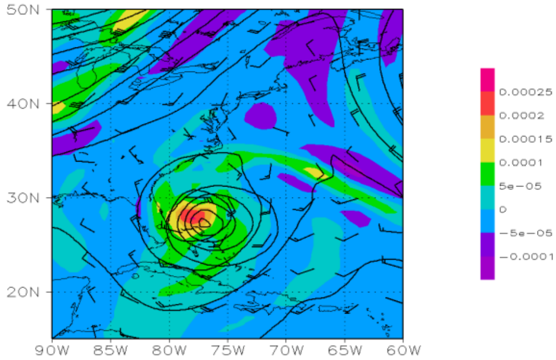

2012-10-27 06UTC

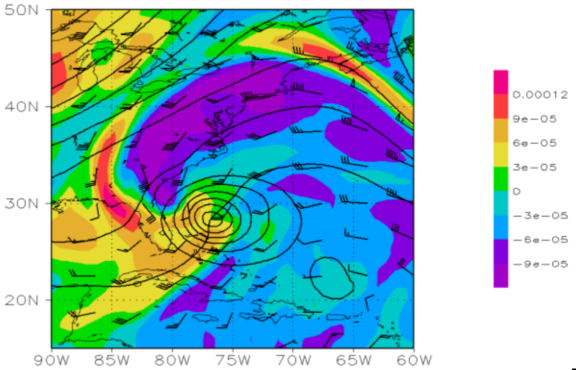

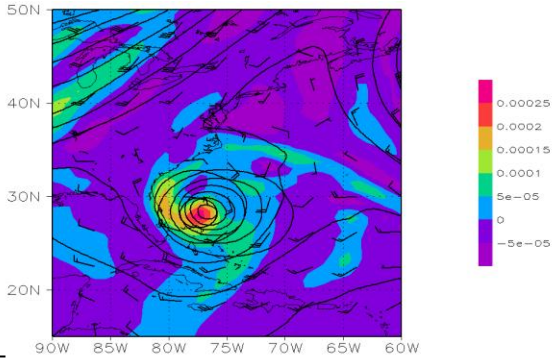

2012-10-27 12UTC

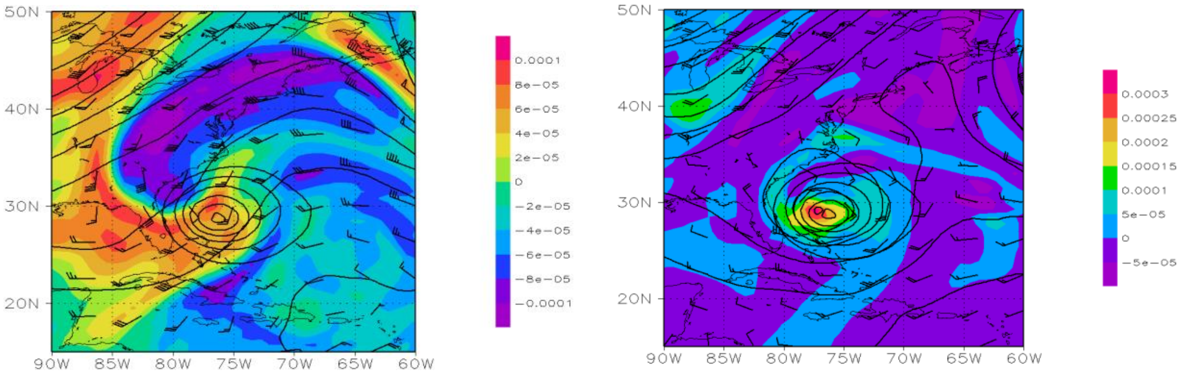

2012-10-27 18UTC

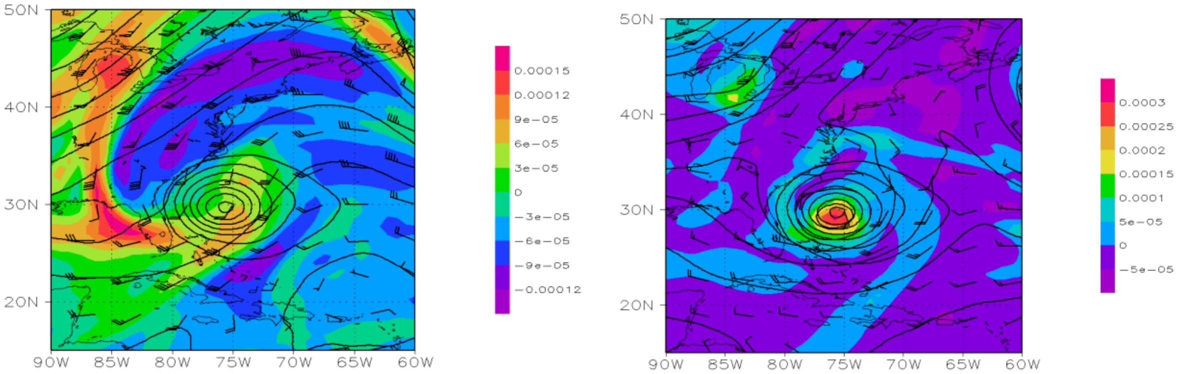

2012-10-28 00UTC

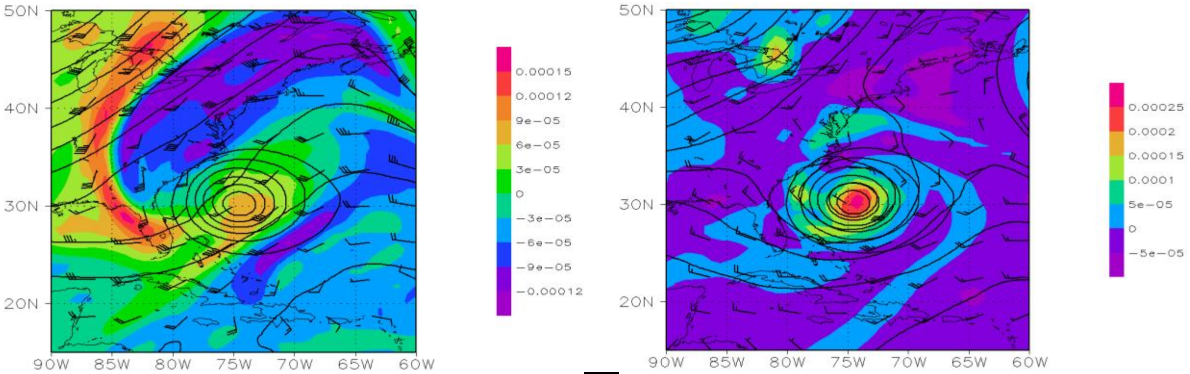

2012-10-28 06UTC

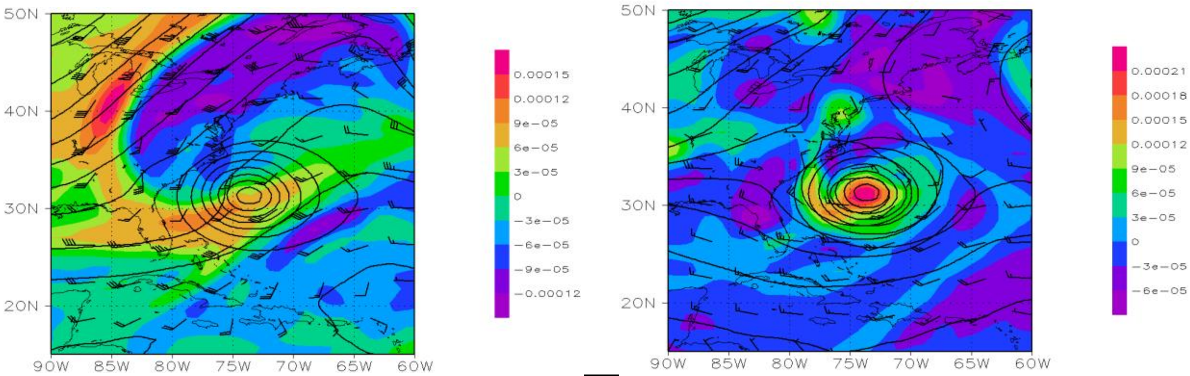

2012-10-28 12UTC

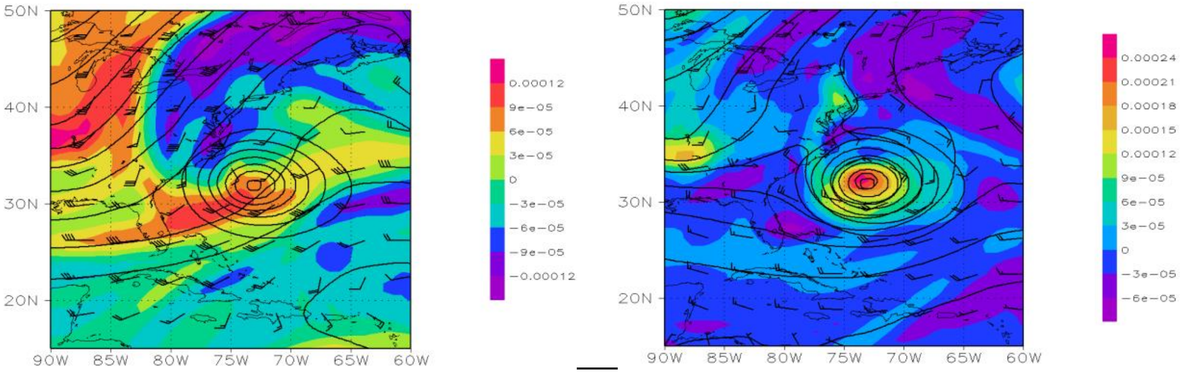

2012-10-28 18UTC

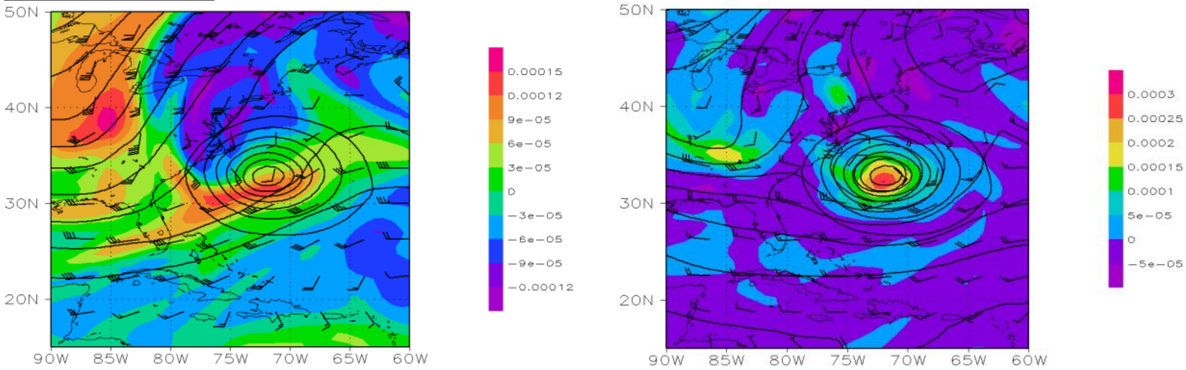

2012-10-29 00UTC

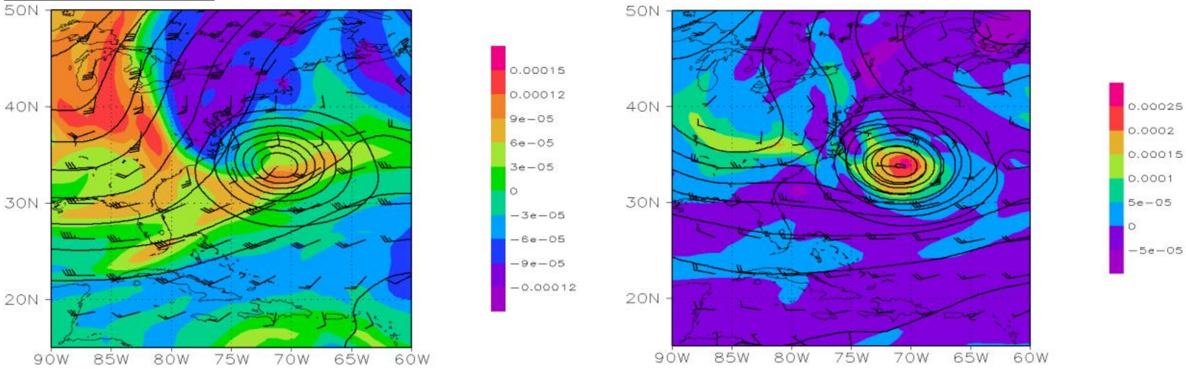

2012-10-29 06UTC

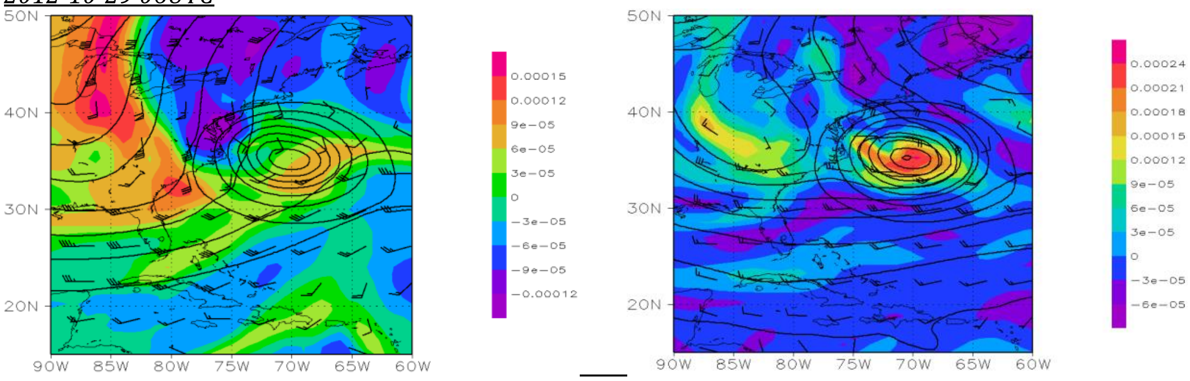

2012-10-29 12UTC

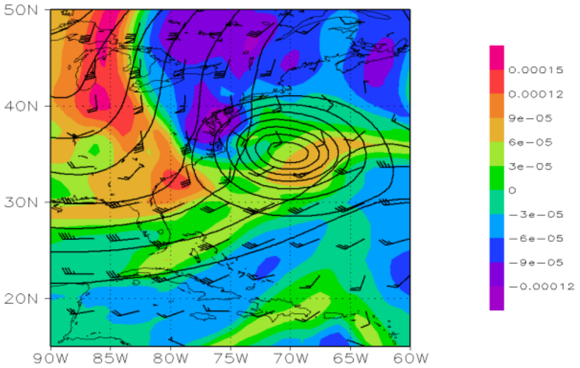

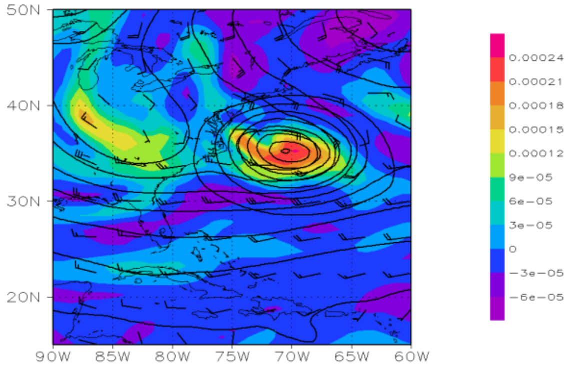

2012-10-29 12UTC

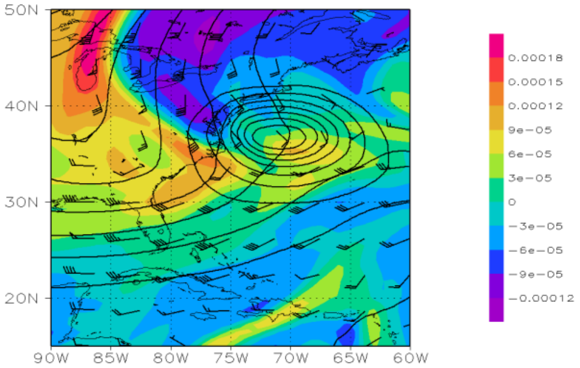

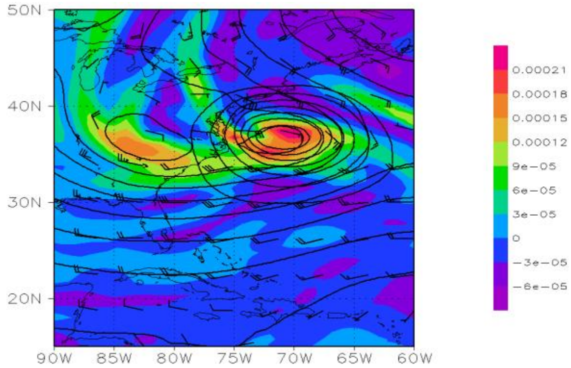

Values and Data from the National Hurricane Center

Date/Time (UTC)	Latitude (°N)	Longitude (°W)	Pressure (mb)	Wind Speed (kt)	Stage
21/1800	14.3	77.4	1006	25	Low
22/0000	13.9	77.8	1005	25	″
22/0600	13.5	78.2	1003	25	″
22/1200	13.1	78.6	1002	30	Tropical depression
22/1800	12.7	78.7	1000	35	Tropical Storm
23/0000	12.6	78.4	998	40	″
23/0600	12.9	78.1	998	40	″
23/1200	13.4	77.9	995	40	″
23/1800	14.0	77.6	993	45	″
24/0000	14.7	77.3	990	55	″
24/0600	15.6	77.1	987	60	″
24/1200	16.6	76.9	981	65	Hurricane
24/1800	17.7	76.7	972	75	″
24/1900	17.9	76.6	971	75	″
25/0000	18.9	76.4	964	85	″
25/0525	20.0	76.0	954	100	″
25/0600	20.1	76.0	954	100	″
25/0900	20.9	75.7	960	95	″
25/1200	21.7	75.5	966	95	″
25/1800	23.3	75.3	963	90	″
26/0000	24.8	75.9	965	75	″
26/0600	25.7	76.4	968	70	″
26/1200	26.4	76.9	970	65	″
26/1800	27.0	77.2	971	65	″
27/0000	27.5	77.1	969	60	Tropical Storm
27/0600	28.1	76.9	968	60	″
27/1200	28.8	76.5	956	70	Hurricane
27/1800	29.7	75.6	960	70	″
28/0000	30.5	74.7	960	65	″
28/0600	31.3	73.9	959	65	″
28/1200	32.0	73.0	954	65	
28/1800	32.8	72.0	952	65	″
29/0000	33.9	71.0	950	70	″
29/0600	35.3	70.5	947	80	″
29/1200	36.9	71.0	945	85	″
29/1800	38.3	73.2	940	80	″
29/2100	38-8	74.0	943	75	Extratropical
29/2330	39.4	74.4	945	70	″
30/0000	39.5	74.5	946	70	″
30/0600	39.9	76.2	960	55	″
30/1200	40.1	77.8	978	50	″
30/1800	40.4	78.9	986	40	″
31/0000	40.7	79.8	992	35	″
31/0600	41.1	80.3	993	35	″
31/1200	41.5	80.7	995	30	″
31/1800					Dissipated

Values from the report *Tropical Cyclone Report- Hurricane Sandy* Blake *et al.* pp. 24-25.

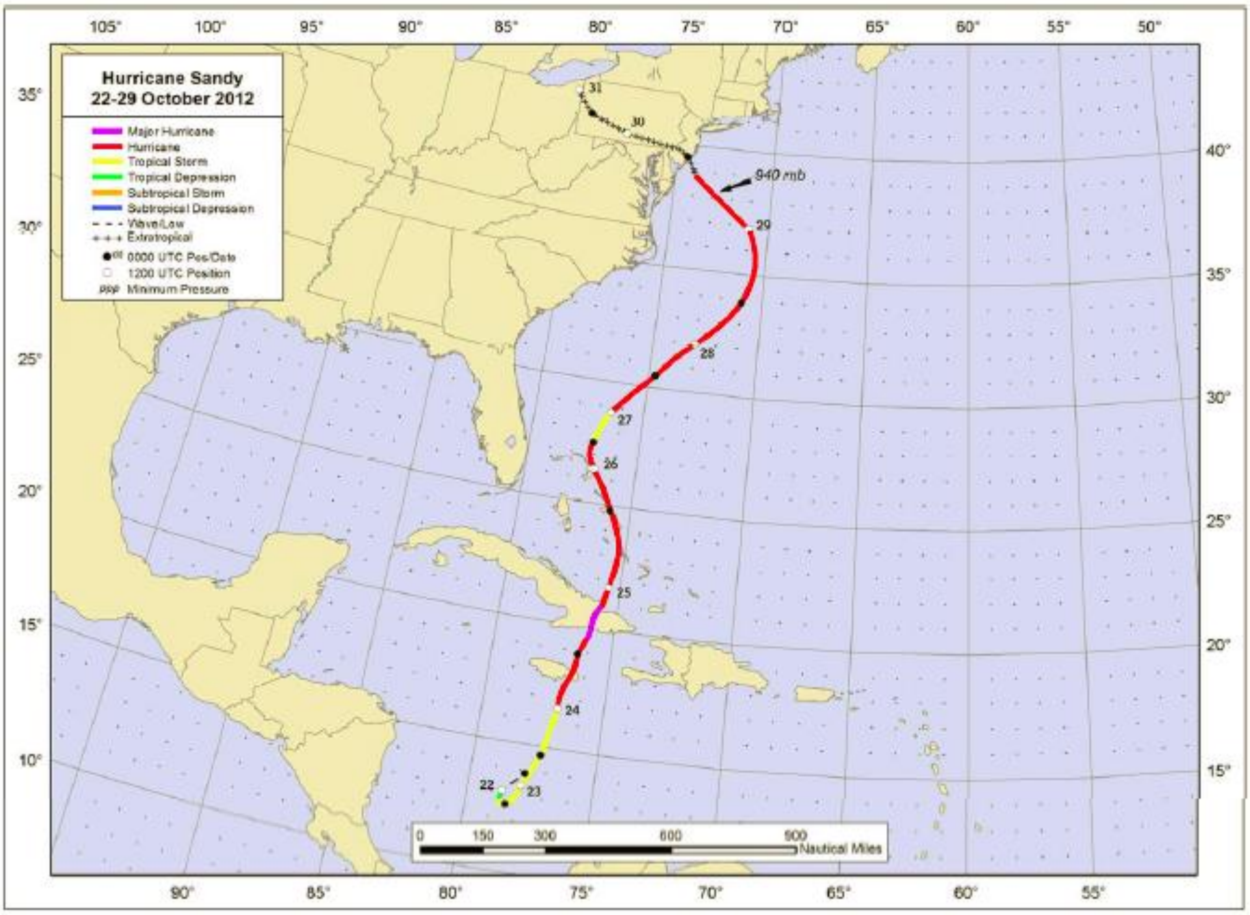

Sandy's track according to NHC. Courtesy to Blake *et al,* 2013.